Outage Analysis of Spectrum-Sharing over M-Block Fading with Sensing Information

AbdulRahman Alabbasi, *Student Member, IEEE*, Zouheir Rezki, *Senior Member, IEEE*, Basem Shihada, *Senior Member, IEEE*

Abstract

Future wireless technologies, such as, 5G, are expected to support a real-time applications with huge data throughput, e.g., holographic meetings. From a bandwidth perspective, cognitive radio is a promising technology to enhance the system's throughput via sharing the licensed spectrum. From a delay perspective, it is well known that increasing the number of decoding blocks will improve the system robustness toward error, while increasing the delay. Therefore, optimally allocating the resources to determine the tradeoff of tuning the length of decoding blocks while sharing the spectrum is a critical topic for future wireless systems. In this work, we minimize the targeted outage probability over the block-fading channels while utilizing the spectrum sharing concept. The secondary user's outage region and the corresponding optimal power are derived, over two-blocks and M-blocks fading channels. We propose two sub-optimal power strategies and derive the associated asymptotic lower and upper bounds on the outage probability with tractable expressions. These bounds allow us to derive the exact diversity order of the secondary user's outage probability. To further enhance the system's performance, we also investigate the impact of including the sensing information on the outage problem. The outage problem, while including the sensing impact, is solved via proposing an alternating optimization algorithm. Selected numerical results are presented to characterize the system's behavior and show the added improvements of several sharing concepts.

Index Terms

Block-Fading channel, outage probability, resource allocation, spectrum-sharing, spectrum-sensing, alternating algorithm.

I. INTRODUCTION

The demand for reliable and real-time communication systems with huge data rate has increased due to the improvement in quality of services of the communications applications, e.g., video streaming for mobile devices and holographic meetings, [1]. This magnifies the necessity of studying delay-limited performance in real-time systems while maintaining large data rate. It is well known that decoding longer codewords of the received message increases the system's robustness toward noise and interference, thus improving system reliability. However, such decoding increases the receiving delay, which prevents widespread deployment of real-time communication systems. Therefore, studying Block-Fading (BF) models is essential to tackle and characterize delay-limited, real-time, systems [3], [4]. In BF models, a message is encoded into M codewords or blocks, i.e., one frame, each block undergoes different fading. Each codeword comprises N symbols that undergo a similar fading gain. These M blocks are separated by frequency, e.g., Orthogonal-Frequency-Division-Multiplexing (OFDM), time, e.g., Time-Division-Multiple-Access (TDMA), or both [2]. The outage probability metric over BF channels is an important measure in delay-limited systems with fixed communication rates [5]. In the context of frame error rate, minimizing the outage probability leads to minimizing the number of average retransmissions of media access control frames. On the other hand, increasing the system's throughput requires an increase in the bandwidth, power, number of operating antennas, etc. Accessing the inefficiently utilized licensed spectrum is a key enabler concept to enhance the system's throughput, i.e., spectrum sharing. This concept is realized by adopting the cognitive radio (CR) technology. CR allows the un-licensed users (secondary users (SUs)) to dynamically access the allocated bands of licensed users (primary users (PUs)) to increase their bands and throughput [6]. Spectrum sharing can be performed via several approaches, such as, opportunistic sharing, overlaying sharing, and underlaying sharing. The opportunistic approach forces the secondary user (SU) to sense the primary user (PU)s spectrum holes, i.e., unused PU bands, and only transmit on these bands when they are unused by the PU. The overlaying sharing approach is considered when PU allows SU to use portion of PU's bandwidth for some time or over a certain geographical area in exchange for obtaining assistant from the SU, e.g., SU

relays PU's signal. Finally, the underlaying approach is when the PU allows the SU to transmit on its bands within a certain tolerable interference threshold [7], [8], [9]. BF-based CR systems that utilize the outage metric, as an evaluation measure, is of extreme interest to be analyzed before the deployment of real-time future systems [10], [11], [12], [13]. This paper analyzes the outage performance of the secondary system over M-block fading under several spectrum sharing scenarios and sensing information.

The problem of characterizing the outage over BF channels has been thoroughly investigated. Authors of [5] tackled the minimization of the outage probability under long-term and short-term power constraints with perfect knowledge of the transmitter-receiver channel state information (CSI). However, they did not consider an interference channel. In [14], authors derived the outage performance of a multiple antenna BF system with delay and power limitation constraints and proposed a coding scheme that minimizes the outage probability of the system. Minimizing the average transmission power under an information outage constraint of the BF channels with acausal knowledge of the channel is investigated in [15]. The analysis of the outage performance of a two-user cognitive radio model is investigated in [16], where acausal knowledge of the message of the PU is known at the SU side. In [17], authors tackled the problems of maximizing the ergodic capacity and maximizing the service outage capacity in a CR environment subject to the PU's outage constraints and SU's power and outage constraints. They assumed a multi-carrier system with a perfect knowledge of both the PU's transmission power policy and the entire network's channels gains. Without a constraint on the number of decoding blocks, authors of [18] derived the optimal power to maximize ergodic capacity and minimize outage capacity. This analysis is conducted while protecting the PU by limiting its outage to a certain threshold. In [19], authors tackled the minimization of two type of outage probability, i.e., group outage and individual outage probabilities under a CR multi-cast network. They also considered the rate/power design of the minimization of weighted aggregated outage probability. Considering the sensing overhead, authors of [20] have addressed the minimization of outage probability in a Rayleigh fading channel. They also showed the improvement gained by introducing the cognitive relay concept. Authors of [21] have defined a probability of instantaneous bit error

outage, i.e., the probability of the instantaneous bit error probability exceeds a certain threshold. They proposed a power control scheme that adapts the transmission power according to the channel state to guarantee a certain quality of service (QoS).

In this work, we consider an M block-fading channels under CR environment. Our main objective is to minimize the targeted SU's outage probability and derive the corresponding optimal adaptive power. We analyze the impact of different spectrum sharing scenarios on the minimum outage problem, i.e., underlaying sharing and combined opportunistic and underlaying sharing. In the first scenario, we consider the case where PU is always active, thus, we do not include sensing information. In the second scenario, we consider that PU activity follows a probabilistic model. Thus, we utilize an SU's sensor to sense if PU's is active or idle, consequently SU transmits with different optimal power policy. We consider several constraints under each scenario: short-term power, long-term power, and CR constraints. The short-term power constraint limits the transmission power over M blocks to a certain threshold. In practice, this constraint ensures that the linear power amplifier does not operate in the saturation region and remains in the linear amplification region. The long-term power constraint forces the expected value of the frame power to be less than a certain threshold. This constraint preserves the transmitter's battery life. The CR constraint represents the effect of secondary transmission on the PU's outage probability.

In this work, we have several assumptions. The PU operates in a stringent delay-limited mode and thus decodes its message over a single block and decodes interference as noise. Both secondary transmitter (ST) and secondary receiver (SR) share the CSI of their instantaneous channel gain, whereas only the statistical CSI of the cross-link between the secondary's and the primary's channel is made available. These assumptions place the system closer to practical scenarios since SU systems seldom know the CSI and power policies of PU systems. The use of the outage metric also underscores the practicality of the proposed system, since it characterizes the real-time performance of a communication system.

Considering the above system characteristics, we summarize our contributions through out the paper as follows.

- We derive an optimal power policy that minimizes SU's targeted outage probability over the M blocks in addition to expressing the corresponding outage region.
- We present explicit expressions of the corresponding outage region and optimal power for $M = 2$. This example shows the complexity of the explicit solutions. We therefore propose two sub-optimal power strategies.
- We verify that the corresponding outage probabilities of these sub-optimal power strategies, have tractable expressions, are the lower and upper bounds on the targeted outage probability.
- By utilizing the above mentioned bounds we derive the diversity order of the exact system.
- We show that the sub-optimal power strategies of the asymptotic lower bound is optimal in the high power regime. Note that all the above mentioned contributions have been conducted while considering the underlaying sharing scenario.
- We analyze the effect of sensing the generalized activity of PU, second scenario, on the SU's outage performance, which is proven to improve the system's outage probability performance, in compared with the first scenario. This results in a complex problem that cannot be solved with conventional methods, due to the non-convex and non-linear structure of the problem.
- We are the first to prove that the weighted sum of the outage probability metrics (under BF channel) is strictly quasi-convex function. We utilized this fact and consequently propose an alternating optimization (AO) algorithm to guarantee the global optimal solution.
- We derive the minimum outage region and the corresponding optimal power, after including the SU's sensing information (about the PU).
- We present selected numerical results to show the effect of the CR constraint and sensing information on the performance yardstick, in addition to comparing between different sharing scenarios.

Unlike the work in [22] and [17], where the knowledge on the instantaneous CSI of all network channels is made available to all terminals, our work captures a more practical scenario where the cross-link between the ST and the primary receiver (PR) is unknown, i.e., only a statistical knowledge is required. They also do not consider the outage probability as a targeted objective

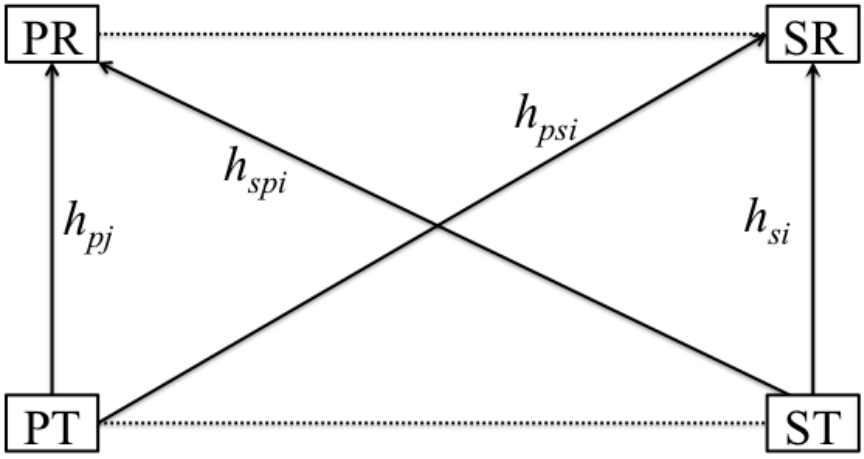

Fig. 1: The system model showing the i-th block of the SU's link, j-th block of the PU's link, and the corresponding cross-links.

to be minimized. Our proposal also differs from that in [5] by considering an interference and sharing environment.

The rest of the paper is organized as follows. Section II describes the system model and a summary of a related background. Section III discusses the SU outage problem formulation and its optimal power allocation in an underlaying sharing scenario. Section IV derives the explicit formulas of the outage region and power allocation of a two block-fading case. Section V shows the sub-optimal strategies (upper and lower bounds on the outage probability) and then derives the diversity order of the exact system outage. The sensing information impact on the outage probability analysis is addressed in Section VI. Numerical results are presented in Section VII.

II. System Model & Related Background

A. System Model

We consider a two-user CR system in which both users communicate through a block-fading channel. Fig. 1 depicts the system model during the i^{th} SU block and the j^{th} PU block, $i \in \{1, ..., M\}$, $j \in \{1, ..., K\}$, where M and K are the number of blocks in the SU and PU frames, respectively. In Fig. 1, the fading channels between the primary transmitter (PT) and PR, ST and SR, ST and PR, and PT and SR are designated as h_{pj}, h_{si}, h_{spi}, and h_{psi}, respectively. Note that the corresponding channel gains are the square modulus of the channels, i.e., $\gamma_{pj} = |h_{pj}|^2$, $\gamma_{si} = |h_{si}|^2$, $\gamma_{spi} = |h_{spi}|^2$, $\gamma_{psi} = |h_{psi}|^2$. The channel gain vectors are

expressed as $\boldsymbol{\gamma}_p = \{\gamma_{p1}, \gamma_{p2}, ..., \gamma_{pK}\}$, $\boldsymbol{\gamma}_s = \{\gamma_{s1}, \gamma_{s2}, ..., \gamma_{sM}\}$, $\boldsymbol{\gamma}_{sp} = \{\gamma_{sp1}, \gamma_{sp2}, ..., \gamma_{spM}\}$, $\boldsymbol{\gamma}_{ps} = \{\gamma_{ps1}, \gamma_{ps2}, ..., \gamma_{psM}\}$. The channels h_{pj}, h_{si}, h_{spi}, and h_{psi} are assumed to be independent random variables with continuous and bounded probability density functions (PDFs) and variances σ_p^2, σ_s^2, σ_{sp}^2, and σ_{ps}^2, respectively. For simplicity, PU is assumed to operate in a stringent delay-limited constraint and thus must encode/decode over a single fading block, i.e., $K = 1$.

The received signal at the SR is expressed as follows,

$$y_{si} = h_{si}x_{si} + h_{psi}x_p + n_i, \quad \forall i \in \{1, \ldots, M\}, \tag{1}$$

where x_{si} and x_p are the transmitted secondary and primary signals. The Additive-White-Gaussian-Noise (AWGN) is expressed as n_i. It is assumed that ST and SR share perfect and casual CSI of γ_{si}, $i = 1, \ldots, M$, through a low-rate, error-free, and limited-delay feedback link. We assume a statistical CSI of γ_{spi} at ST. The SU minimizes its outage probability via power adaptation while maintaining a fixed communication rate. It is assumed that PU decodes interference as noise. This is because PU does not have access to the CSI of γ_{spi}. It is also assumed that PU's transmission power has a peak constraint, $\mathcal{P}_p$. This enables us to consider the worst-case scenario of interference toward SU. On the other hand, SU adapts its power with each channel gain, γ_{si} and the effect of PU transmission on SU is also considered in our framework.

Notation: Note that a bold small letter indicates a vector, i.e., $\mathbf{a} = \{a_1, a_2, \ldots, a_M\}$, where M is the vector length. The operator $\mathbb{E}\{.\}$ is the expectation of its argument. The operators $\leq$ and $\geq$ are element-wise operators (unless mentioned otherwise), i.e., $\mathbf{a} \geq 0$ means that all elements of vector $\mathbf{a}$ are greater than or equal to zero. All other notations and terminologies used throughout this paper are defined in Table I.

B. Related Background

In this section, we present a benchmark system to our proposal that will be explained in later sections. We briefly describe the minimum outage probability over M fading blocks along with optimal power adaptation derived in [5]. While in [5], authors did not address the communication in a spectrum-sharing scenario, it is of interest, here, to give an overview of the results therein to highlight the solution structure. Their system is clearly a point-to-point communication system.

TABLE I: Model's Notations

Symbol/Operation	Descriptions	Symbol/Operation	Descriptions
$\langle \mathbf{a} \rangle$	$\langle \mathbf{a} \rangle = \frac{1}{M} \sum_{i=1}^{M} a_i$	$a < b \iff c < d$	The inequality of the left side implies that on the right side and vice versa.
$[a]_c^b$	$\min(\max(a, c), b)$	$a \approx b$	If $\lim_{P \to \infty} \frac{a}{b} \approx 1$, P is transmission power
$\mathcal{P}^{st}$	Short term power threshold	$\mathcal{P}^{lt}$	Long term power threshold
$\mathcal{P}_p$	PU's transmission power	P_s	SU's transmission power
R_s	SU's fixed rate	R_p	PU's fixed rate
ϵ	PU's outage tolerance threshold	α_1 & α_0	Probability of PU active & idle
PT	Primary transmitter	BF	Block-Fading
PR	Primary receiver	OFDM	Orthogonal-Frequency-Division-Multiplexing
ST	Secondary transmitter	TDMA	Time-Division-Multiple-Access
SR	Secondary receiver	CR	Cognitive radio
PU	Primary user	CSI	Channel state information
SU	Secondary user	QoS	Quality of service
$\boldsymbol{\gamma}_{sp}$	ST-to-PR channel gain	CDF	Cumulative density function
$\boldsymbol{\gamma}_{ps}$	PT-to-SR channel gain	AO	Alternating optimization
$\boldsymbol{\gamma}_s$	SU's channel gain	AWGN	Additive-White-Gaussian-Noise
$\boldsymbol{\gamma}_p$	PU's channel gain	i.i.d.	Independent and identicaly distributed
PDF	Probability density function	SINR	Signal-to-Interference-Noise-Ratio

The objective of problem $\mathfrak{P}_0$ is to minimize SU's outage probability over M blocks, while constrained by: short-term and long-term power constraints. Problem $\mathfrak{P}_0$ is defined as:

$$\mathfrak{P}_0 : \quad \min_{\mathbf{p}(\boldsymbol{\gamma}_s)} \Pr\left[\mathcal{I}_M\left(\mathbf{p}\left(\boldsymbol{\gamma}_s\right), \boldsymbol{\gamma}_s\right) < R_s\right] \tag{2a}$$

$$\text{s.t. } \mathfrak{C}_1 : \ \langle \mathbf{p}\left(\boldsymbol{\gamma}_s\right) \rangle \leq \mathcal{P}^{st} \tag{2b}$$

$$\mathfrak{C}_2 : \ \mathbb{E}\{\langle \mathbf{p}\left(\boldsymbol{\gamma}_s\right) \rangle\} \leq \mathcal{P}^{lt}, \tag{2c}$$

where $\mathcal{I}_M\left(\mathbf{p}\left(\boldsymbol{\gamma}_s\right), \boldsymbol{\gamma}_s\right) = \frac{1}{M} \sum_{i=1}^{M} \frac{1}{2} \log\left(1 + p_i(\gamma_{si})\gamma_{si}\right)$ is the SU's mutual information over a single frame. The SU's fixed rate is R_s. The adaptive transmission power is designated as $\mathbf{p}\left(\boldsymbol{\gamma}_s\right)$. The short-term constraint, in (2b), limits the transmission power over one frame to $\mathcal{P}^{st}$. The long-term constraint, in (2c), enforces the expected value of the transmitted power per frame to $\mathcal{P}^{lt}$. It is assumed that $\mathcal{P}^{lt} < \mathcal{P}^{st}$. This assumption is intuitively valid given that in the opposite case, i.e., $\mathcal{P}^{lt} > \mathcal{P}^{st}$, the long-term constraint becomes inactive.

We begin by stating some definitions. Let $\mathcal{Q}$ be the region defined by ordering the channel gains, in a descending order, as follows,

$$\mathcal{Q} = \{\boldsymbol{\gamma}_s \in \mathbb{R}_+^M : \gamma_{s1} \geq \cdots \geq \gamma_{sM}\}. \tag{3}$$

A budget power is defined as a combination of both $\mathfrak{C}_1$ and $\mathfrak{C}_2$ constraints, expressed as follows,

$$\hat{s} = \min\left(\mathcal{P}^{st}, s^*\right), \tag{4}$$

where s^* is understood as an instantaneous power threshold that reflects the effect of the long-term power constraint, $\mathfrak{C}_2$. The value of s^* is obtained by solving the following equality,

$$\int_{\overline{\mathcal{R}}(s^*)} \langle \mathbf{p}(\boldsymbol{\gamma}_s)\rangle dG(\boldsymbol{\gamma}_s) = \mathcal{P}^{lt}, \tag{5}$$

where $G(\boldsymbol{\gamma_s})$ is the cumulative density function (CDF) of $\boldsymbol{\gamma_s}$, and $\overline{\mathcal{R}}(s^*)$ is the no-outage region defined as follows,

$$\overline{\mathcal{R}}(s) = \{\boldsymbol{\gamma}_s \in \mathbb{R}_+^M; \langle \mathbf{p}(\boldsymbol{\gamma}_s)\rangle \leq s\}. \tag{6}$$

The optimal power allocation of $\mathfrak{P}_0$ is expressed as follows,

$$\mathbf{p}^*\left(\boldsymbol{\gamma}_s\right) = \begin{cases} \mathbf{p}^{st}\left(\boldsymbol{\gamma}_s\right); & \text{if} \quad \boldsymbol{\gamma}_s \notin \mathcal{U}(R_s, \hat{s}) \\ 0; & \text{if} \quad \boldsymbol{\gamma}_s \in \mathcal{U}(R_s, \hat{s}) \end{cases}, \tag{7}$$

where $\mathbf{p}^{st}(\boldsymbol{\gamma}_s)$ is obtained by solving the dual problem of (2), i.e., maximizing the mutual information subject to the same short-term constraint in (4). The associated Lagrangian function of the maximization problem is expressed as,

$$\mathcal{L}_{st}\left(\mathbf{p}^{st}\right) = \mathcal{I}_M\left(\mathbf{p}^{st}\left(\boldsymbol{\gamma}_s\right), \boldsymbol{\gamma}_s\right) - \lambda^{st}\left[\langle \mathbf{p}^{st}\left(\boldsymbol{\gamma}_s\right)\rangle - \min\left(\mathcal{P}^{st}, s^*\right)\right]. \tag{8}$$

Finding the zeros of $\frac{\partial \mathcal{L}_{st}\left(\mathbf{p}^{st}\right)}{\partial \mathbf{p}^{st}(\boldsymbol{\gamma}_s)} = 0$ will leads to the following expression of $\mathbf{p}^{st}(\boldsymbol{\gamma}_s)$,

$$p_m^{st}(\boldsymbol{\gamma}_s) = \left[\lambda^{st}(\mu, \boldsymbol{\gamma}_s) - \frac{1}{\gamma_{sm}}\right]_0 \qquad \forall m \in \{1, \ldots, M\}. \tag{9}$$

The Lagrangian multiplier is obtained as,

$$\lambda^{st}(\mu, \boldsymbol{\gamma}_s) = \frac{1}{\mu}\sum_{l=1}^{\mu}\frac{1}{\gamma_{sl}} + \frac{M}{\mu}\hat{s}, \tag{10}$$

where the derivation of this Lagrangian multiplier is obtained by minimizing the Lagrangian function of the dual problem (with respect to λ^{st}), while substituting the optimal power term (7), as shown in Proposition 3 and Appendix B of [5]. The parameter μ is the unique integer

in $\{1,\ldots,M\}$, such that $\lambda_s^{lt}(\mu,\boldsymbol{\gamma}_s) \geq \frac{1}{\gamma_{sm}}$ for $m \leq \mu$ and $\lambda_s^{lt}(\mu,\boldsymbol{\gamma}_s) < \frac{1}{\gamma_{sm}}$ for $m > \mu$. The corresponding outage region is designated as $\mathcal{U}(R_s,\hat{s})$. It is more convenient to show the outage region as the intersection with $\mathcal{V}_\mu$, such that,

$$\mathcal{U}(R_s,\hat{s}) \cap \mathcal{V}_\mu = \left\{\boldsymbol{\gamma}_s \in \mathcal{Q}:\ \frac{1}{M}\sum_{m=1}^{\mu}\frac{1}{2}\log\left(1+\gamma_{sm}p_m^{st}(\boldsymbol{\gamma}_s)\right) < R_s\right\}, \tag{11}$$

The region $\mathcal{V}_\mu$ is a sub-region of $\mathcal{Q}$, defined such that the corresponding power elements are positive, i.e., $\{p_1^{st}(\boldsymbol{\gamma}_s),\ldots,p_\mu^{st}(\boldsymbol{\gamma}_s)\} > 0$. The outage region in (11) satisfies the minimum fixed rate, whereas both the short-term and long-term power constraints are already satisfied through the design of $p_m^{st}(\boldsymbol{\gamma}_s)$. Note that the outage region is equal to the complement of the no-outage region, i.e., $\mathbb{R}_+^M - \overline{\mathcal{R}}(\hat{s})$, where the optimal power associated with $\overline{\mathcal{R}}(\hat{s})$ is given in [5].

III. Minimum Outage Probability in the CR Framework

In this section, the SU's outage probability problem is formulated under the CR environment. The objective of this problem is to minimize the SU's outage probability over BF channels, subject to the short-term power constraint, the long-term power constraint, and the PU's outage constraint (the CR constraint). Both the short-term and long-term power constraints are described in Section II-B. The CR constraint manifests the effect of a multi-block SU communication system on a single-block PU communication system. Assuming that PU operates in a delay-limited mode, thus the PU is protected from SU interference by limiting the PU's outage probability to a certain threshold. Due to the interference of PU, in (1), the exact mutual information of the SU is difficult to compute. We therefore consider a lower bound on the mutual information of the SU, i.e., $\mathcal{I}_M^{(s)}\left(\mathbf{p}_s\left(\boldsymbol{\gamma}_s\right),\boldsymbol{\gamma}_s\right) \geq \mathcal{I}_M^{(s-)}\left(\mathbf{p}_s\left(\boldsymbol{\gamma}_s\right),\boldsymbol{\gamma}_s\right)$, where $\mathbf{p}_s\left(\gamma_s\right)$ is the SU's transmission power. The expression of $\mathcal{I}_M^{(s-)}\left(\mathbf{p}_s\left(\boldsymbol{\gamma}_s\right),\boldsymbol{\gamma}_s\right)$ is derived along similar lines as in [23], i.e.,

$$\mathcal{I}_M^{(s-)}\left(\mathbf{p}_s\left(\boldsymbol{\gamma}_s\right),\boldsymbol{\gamma}_s\right) = \frac{1}{2M}\sum_{i=1}^{M}\log\left(1+\frac{p_{si}\left(\boldsymbol{\gamma}_s\right)\gamma_{si}}{1+\mathcal{P}_p\sigma_{ps}^2}\right). \tag{12}$$

Consequently, the upper bound of the exact outage probability is $P_{out}^{+} = \Pr\left[\mathcal{I}_M^{(s-)}\left(\mathbf{p}_s\left(\boldsymbol{\gamma}_s\right),\boldsymbol{\gamma}_s\right) < R_s\right]$. Hereafter, P_{out}^{+} is designated as the outage probability of the SU. Note that the term $1+\mathcal{P}_p\sigma_{ps}^2$ is found by considering the worst-case case scenario (where PU transmits with maximum power

$\mathcal{P}_p$ and PU is active all the time) of PT transmission and conducting a short period of spectrum-sensing at the SU side. Likewise, the exact PU mutual information is difficult to compute. Therefore, we formulate the CR constraint using a lower bound on the PU's mutual information, i.e., $\mathcal{I}_i^{(p-)}$. Following similar lines as in [23], given γ_{si} on the SU side, $\mathcal{I}_i^{(p-)}$ is obtained as $\mathcal{I}_i^{(p-)} = \frac{1}{2}\log\left(1+\frac{\mathcal{P}_p\gamma_p}{p_{si}(\gamma_{si})\sigma_{sp}^2+1}\right)$. Note that the condition on γ_{si} follows from the fact that we enforce the corresponding PU outage constraint on the SU's side. Recall that γ_p is known on the PU's side and γ_{si} is known on SU's. It follows that the PU's outage probability constraint is upper bounded by $\Pr\left[\mathcal{I}_i^{(p-)} < R_p \middle| \gamma_{si}\right]$. The fixed rate of PU is designated as R_p. The proposed problem, $\mathfrak{P}_1$, is formulated as follows,

$$\mathfrak{P}_1: \quad \min_{\mathbf{p}_s(\boldsymbol{\gamma}_s)} \Pr\left[\mathcal{I}_M^{(s-)}\left(\mathbf{p}_s\left(\boldsymbol{\gamma}_s\right),\boldsymbol{\gamma}_s\right) < R_s\right] \tag{13a}$$

$$\text{s.t.} \;\; \mathfrak{C}_1: \; \langle \mathbf{p}_s\left(\boldsymbol{\gamma}_s\right)\rangle \leq \mathcal{P}^{st} \tag{13b}$$

$$\mathfrak{C}_2: \; \mathbb{E}\{\langle \mathbf{p}_s\left(\boldsymbol{\gamma}_s\right)\rangle\} \leq \mathcal{P}^{lt} \tag{13c}$$

$$\mathfrak{C}_{3i}: \; \Pr\left[\mathcal{I}_i^{(p-)} < R_p \middle| \gamma_{si}\right] \leq \epsilon, \; \forall \; i \in \{1,...,M\}. \tag{13d}$$

The constant ϵ is PU's tolerance in terms of its QoS due to the effect of ST's interference. The formulation of (13) is motivated from the fact that a realistic CR environment must take into account several implementation factors. The impact of the PU interference toward the SU is an important factor, reflected in the expression of SU's mutual information in (13a). The impact of the underlaying sharing on the PU's outage performance, which is formulated in constraint (13d).

In order to solve $\mathfrak{P}_1$, we note that constraint (13d) can be converted to an instantaneous power constraint as follows, $\mathfrak{C}_{3i}$:

$$\Pr\left[\frac{1}{2}\log\left(1+\frac{\mathcal{P}_p\gamma_p}{p_{si}(\gamma_{si})\sigma_{sp}^2+1}\right) < R_p \middle| \gamma_{si}\right] \leq \epsilon \implies F_{\gamma_p|\gamma_{si}}\left(\frac{\left(p_{si}(\gamma_{si})\sigma_{sp}^2+1\right)\left(e^{2R_p}-1\right)}{\mathcal{P}_p}\right) \leq \epsilon \tag{14a}$$

$$\implies p_{si}\left(\gamma_{si}\right) \leq \left[\frac{F_{\gamma_p|\gamma_{si}}^{-1}\left(\epsilon\right)\mathcal{P}_p}{(e^{2R_p}-1)\sigma_{sp}^2} - \frac{1}{\sigma_{sp}^2}\right]_0 = \mathcal{P}_{pu}, \tag{14b}$$

where (14b) results from the independence between γ_p and γ_{si} and from the fact that $F_{\gamma_p|\gamma_{si}}$, being a CDF, is a monotonically non-decreasing function, note that its inverse is also non-decreasing. Note that $\mathcal{P}_{pu}$ increases with both ϵ and $\mathcal{P}_p$ and decreases with R_p.

The solution of problem $\mathfrak{P}_1$ contains the effect of constraint $\mathfrak{C}_{3i}$ and the interference from

PT. The optimal power allocation of $\mathfrak{P}_1$ is expressed as follows,

$$\hat{\mathbf{p}}_s(\boldsymbol{\gamma}_s) = \min\left(\mathbf{p}_s^*(\boldsymbol{\gamma_s}), \mathcal{P}_{pu}\right), \tag{15}$$

where the function $\min\left(\mathbf{p}_s^*(\boldsymbol{\gamma_s}), \mathcal{P}_{pu}\right)$ is an element-wise function of $\mathbf{p}_s^*(\boldsymbol{\gamma_s})$. The power profile, $\mathbf{p}_s^*(\boldsymbol{\gamma_s})$, is expressed as follows,

$$\mathbf{p}_s^*\left(\boldsymbol{\gamma}_s\right) = \begin{cases} \mathbf{p}_s^{st}\left(\boldsymbol{\gamma}_s\right); & \text{if} \quad \boldsymbol{\gamma}_s \notin \mathcal{U}_{cr}(R_s, \hat{s}) \\ 0; & \text{if} \quad \boldsymbol{\gamma}_s \in \mathcal{U}_{cr}(R_s, \hat{s}) \end{cases}, \tag{16}$$

where $\mathbf{p}_s^{st}(\boldsymbol{\gamma}_s)$ is formulated as follows,

$$p_{sm}^{st}(\boldsymbol{\gamma}_s) = \left[\lambda_s^{st}(\mu, \boldsymbol{\gamma}_s) - \frac{1 + \mathcal{P}_p\sigma_{ps}^2}{\gamma_{sm}}\right]_0 \qquad \forall m \in 1, \ldots, M. \tag{17}$$

Recall that $\hat{s} = \min\left(\mathcal{P}^{st}, s^*\right)$ and s^* is defined such that,

$$\int_{\overline{\mathcal{R}_{cr}}(s^*)} \langle \mathbf{p}_s(\boldsymbol{\gamma}_s)\rangle dG(\boldsymbol{\gamma}_s) = \mathcal{P}^{lt}, \tag{18}$$

where $\overline{\mathcal{R}_{cr}}(\hat{s}) = \{\boldsymbol{\gamma}_s \in \mathbb{R}_+^M; \langle \hat{\mathbf{p}}_s(\boldsymbol{\gamma}_s)\rangle \leq \hat{s}\}$. It is more convenient to define the SU outage region, designated as $\mathcal{U}_{cr}(R_s, \hat{s})$, as the union of the outage region intersection with each of the positive power regions, i.e., $\bigcup_{\mu=1}^{M} \mathcal{U}_{cr}(R_s, \hat{s}) \cap \mathcal{V}_\mu$. Each of these intersections is defined as follows,

$$\mathcal{U}_{cr}(R_s, \hat{s}) \cap \mathcal{V}_\mu = \left\{\boldsymbol{\gamma}_s \in \mathcal{Q} : \ \frac{1}{2M}\sum_{m=1}^{\mu} \log\left(1 + \frac{\gamma_{sm}\hat{p}_{sm}(\boldsymbol{\gamma}_s)}{1 + \mathcal{P}_p\sigma_{ps}^2}\right) < R_s\right\}, \tag{19}$$

where the Lagrangian multiplier

$$\lambda_s^{st}(\mu, \boldsymbol{\gamma}_s) = \frac{1 + \mathcal{P}_p\sigma_{ps}^2}{\mu}\sum_{l=1}^{\mu}\frac{1}{\gamma_{sl}} + \frac{M}{\mu}\hat{s}, \tag{20}$$

where the derivation of the Lagrangian multiplier is done in similar lines to that in (10) and a similar one in [5]. The region $\mathcal{V}_\mu$ is a sub-region of $\mathcal{Q}$, defined such that the corresponding power elements are positive, i.e., $\{p_{s1}^{st}(\boldsymbol{\gamma}_s), \ldots, p_{sv}^{st}(\boldsymbol{\gamma}_s)\} \geq 0$. The integer μ is the unique number in $\{1, \ldots, M\}$, such that $\frac{\left(1+\mathcal{P}_p\sigma_{ps}^2\right)}{\gamma_{sm}} \leq \lambda_s^{st}$ for $m \leq \mu$ and $\frac{\left(1+\mathcal{P}_p\sigma_{ps}^2\right)}{\gamma_{sm}} > \lambda^{st}$ for $m > \mu$.

Note that the outage region in (19) differs from the region in (11) by the effect of the CR instantaneous power constraint, $\mathcal{P}_{pu}$, and PT's interference, $\mathcal{P}_p\sigma_{ps}^2$.

The complexity of computing the above outage region and its associated probability increases

with the number of blocks, M. Below, we provide an example to show this complexity.

IV. Application For $M = 2$

In this section, we formulate the minimum outage region of problem $\mathfrak{P}_1$ when the number of secondary communication blocks is equal to $M = 2$. Likewise, in the previous section, we provide our solution for an ordered $\mathcal{Q}$, i.e., we assume that $\gamma_{s1} \geq \gamma_{s2}$. The analysis in this section is valid for general channel distributions. To make this section more readable and avoid directly presenting cumbersome mathematics, we divide the derivation into several steps. Steps 1 and 2 are mainly for deriving the outage region. **Step 1** describes the outage region intersection with region $\mathcal{V}_1$, as in (21), where the power is assigned to one block. **Step 2** describes the outage region intersection with region $\mathcal{V}_2$, as in (22), where the power is assigned to both communication blocks. **Step 3** derives the corresponding optimal power allocation over non-outage regions.

In **Step 1**, we derive the intersection of the outage region with region $\mathcal{V}_1$ (i.e., $\mathcal{U}_{cr}\left(R_s, \hat{s}\right) \cap \mathcal{V}_1$), as given in (21). This region is the union of two sub-regions, which are obtained by considering (19), such that, $\frac{1}{4}\log\left(1+\frac{\gamma_{s1}}{P_I}\min\left(\left[\lambda_s^{st}(1,\boldsymbol{\gamma}_s)-\frac{P_I}{\gamma_{s1}}\right],\mathcal{P}_{pu}\right)\right) < R_s$, where $P_I = 1+\mathcal{P}_p\sigma_{ps}^2$. The first sub-region occurs when $\lambda_s^{st}(1,\boldsymbol{\gamma}_s)-\frac{P_I}{\gamma_{s1}} > \mathcal{P}_{pu}$, which leads to $\hat{s} \geq \frac{\mathcal{P}_{pu}}{2}$, which is interpreted as the CR constraint being active. Then, by solving $\frac{1}{4}\log\left(1+\frac{\gamma_{s1}\mathcal{P}_{pu}}{P_I}\right) < R_s$, we obtain, $\gamma_{s1} < \frac{(e^{4R_s}-1)P_I}{\mathcal{P}_{pu}} = z_0$. The second sub-region occurs when $\hat{s} < \frac{\mathcal{P}_{pu}}{2}$ and is interpreted as the CR constraint being inactive. Then, solving $\frac{1}{4}\log\left(1+\frac{\gamma_{s1}}{P_I}\left[\lambda_s^{st}(1,\boldsymbol{\gamma}_s)-\frac{P_I}{\gamma_{s1}}\right]\right) < R_s$, we obtain, $\gamma_{s1} < \frac{P_I(e^{4R_s}-1)}{2\hat{s}} = z_1$. Finally, recall that $\mathcal{V}_1$ requires satisfying $\lambda_s^{st}(1,\boldsymbol{\gamma}_s) < \frac{P_I}{\gamma_{s1}}$. Thus, it leads to $\gamma_{s2} < \frac{P_I\gamma_{s1}}{P_I+2\gamma_{s1}\hat{s}} = \eta_1(\gamma_{s1})$.

$$\mathcal{U}_{cr}(R_s,\hat{s})\cap\mathcal{V}_1 = \Big\{\boldsymbol{\gamma}_s\in\mathcal{Q}:(\hat{s}\geq\frac{\mathcal{P}_{pu}}{2})\cap[\gamma_{s1}<z_0\ \cap\ \gamma_{s2}<\eta_1(\gamma_{s1})]\cup(\hat{s}<\frac{\mathcal{P}_{pu}}{2})\cap[\gamma_{s1}<z_1\ \cap\ \gamma_{s2}<\eta_1(\gamma_{s1})]\Big\}. \tag{21}$$

Step 2. We derive the outage region intersection with $\mathcal{V}_2$, i.e., $\mathcal{U}_{cr}(R_s,\hat{s})\cap\mathcal{V}_2$, given by (22). This region is formulated in terms of three regions (obtained from (19)), $\mathcal{A}$, $\mathcal{B}$, and $\mathcal{C}$, as expressed in (22). The three regions are as follows. The first region is defined as $\mathcal{A} = \left\{\boldsymbol{\gamma}_s \in \mathcal{Q} : \left[p_{s1}\left(\gamma_s\right) \leq \mathcal{P}_{pu}\right] \cap \left[p_{s2}\left(\gamma_s\right) \leq \mathcal{P}_{pu}\right]\right\}$. The second region is formulated as $\mathcal{B} = \left\{\boldsymbol{\gamma}_s \in \mathcal{Q} : \left[p_{s1}\left(\gamma_s\right) > \mathcal{P}_{pu}\right] \cap \left[p_{s2}\left(\gamma_s\right) > \mathcal{P}_{pu}\right]\right\}$. The third region is defined as $\mathcal{C} = \left\{\boldsymbol{\gamma}_s \in \mathcal{Q} : \left[p_{s1}\left(\gamma_s\right) > \mathcal{P}_{pu}\right] \cap \left[p_{s2}\left(\gamma_s\right) \leq \mathcal{P}_{pu}\right]\right\}$. The contributions of $\mathcal{A}$, $\mathcal{B}$, and $\mathcal{C}$ to the outage are

TABLE II: Parameters of all Outage Sub-Regions

Parameters Definition	Parameters Definition
$z_0 = \frac{(e^{4R_s}-1)P_I}{\mathcal{P}_{pu}}$	$z_1 = \frac{P_I(e^{4R_s}-1)}{2\hat{s}}$
$\gamma_{s2} < \frac{P_I\gamma_{s1}}{P_I+2\gamma_{s1}\hat{s}} = \eta_1(\gamma_{s1})$	$z_{a1} = \frac{P_I(e^{2R_s}-1)}{\hat{s}}$
$z_{b1} = \sqrt{\frac{P_I^2 e^{4R_s}}{\mathcal{P}_{pu}^2}} - \frac{P_I}{\mathcal{P}_{pu}}$	$z_{b2} = \frac{P_I e^{4R_s}-P_I}{\mathcal{P}_{pu}}$
$z_{c1} = \frac{1}{2}\sqrt{\frac{\mathcal{P}_{pu}^2P_I^2+4\mathcal{P}_{pu}P_I^2e^{4R_s}\hat{s}-2\mathcal{P}_{pu}P_I^2\hat{s}+P_I^2\hat{s}^2}{\mathcal{P}_{pu}^2\hat{s}^2}} + \frac{-\mathcal{P}_{pu}P_I-P_I\hat{s}}{2\mathcal{P}_{pu}\hat{s}}$	$z_{c2} = \frac{P_I(2e^{4R_s}-1)}{\mathcal{P}_{pu}}$
$\eta_{a2}(\gamma_{s1}) = \frac{-2\gamma_{s1}^2P_I\hat{s}+2\gamma_{s1}P_I^2e^{4R_s}-\gamma_{s1}P_I^2}{(2\gamma_{s1}\hat{s}+P_I)^2} + 2\sqrt{\frac{-2\gamma_{s1}^3P_I^3e^{4R_s}\hat{s}+\gamma_{s1}^2P_I^4e^{8R_s}-\gamma_{s1}^2P_I^4e^{4R_s}}{(2\gamma_{s1}\hat{s}+P_I)^4}}$	$\eta_{a3}(\gamma_{s1}) = \frac{\gamma_{s1}P_I}{2\gamma_{s1}\mathcal{P}_{pu}-2\gamma_{s1}\hat{s}+P_I}$
$\eta_{b2}(\gamma_{s1}) = \frac{-\gamma_{s1}\mathcal{P}_{pu}P_I+P_I^2e^{4R_s}-P_I^2}{\gamma_{s1}\mathcal{P}_{pu}^2+\mathcal{P}_{pu}P_I}$	$\eta_{b3}(\gamma_{s1}) = -\frac{\gamma_{s1}P_I}{2\gamma_{s1}\mathcal{P}_{pu}-2\gamma_{s1}\hat{s}-P_I}$
$\eta_{c2}(\gamma_{s1}) = \frac{-\gamma_{s1}^2\mathcal{P}_{pu}P_I+2\gamma_{s1}P_I^2e^{4R_s}-\gamma_{s1}P_I^2}{2\gamma_{s1}^2\mathcal{P}_{pu}\hat{s}+\gamma_{s1}\mathcal{P}_{pu}P_I+2\gamma_{s1}P_I\hat{s}+P_I^2}$.	

expressed in (23), (24), and (25), respectively. Note that the outage region depends on the relation among $\hat{s}$ and $\mathcal{P}_{pu}$. The parameters of (23), (24), and (25) are derived following similar lines as deriving the parameters in (21). They are defined as follows,

$$\mathcal{U}_{cr}(R_s,\hat{s})\cap\mathcal{V}_2 = \left\{\boldsymbol{\gamma}_s\in\mathcal{Q}:[\mathcal{U}_{cr}(R_s,\hat{s})\cap\mathcal{V}_2\cap\mathcal{A}]\cup[\mathcal{U}_{cr}(R_s,\hat{s})\cap\mathcal{V}_2\cap\mathcal{B}]\cup[\mathcal{U}_{cr}(R_s,\hat{s})\cap\mathcal{V}_2\cap\mathcal{C}]\right\} \quad . \tag{22}$$

$$\begin{aligned}\mathcal{U}_{cr}(R_s,\hat{s})\cap\mathcal{V}_2\cap\mathcal{A} = \Bigg\{&\boldsymbol{\gamma}_s\in\mathcal{Q}:\ (\mathcal{P}_{pu}>\hat{s}\cap\eta_{a3}(\gamma_{s1})\le\gamma_{s2}\le\gamma_{s1})\\ &\bigcap\Big((0<\gamma_{s1}<z_{a1}\cap\eta_1(\gamma_{s1})\le\gamma_{s2}\le\gamma_{s1})\cup(z_{a1}<\gamma_{s1}<z_1\cap\eta_1(\gamma_{s1})\le\gamma_{s2}<\eta_{a2}(\gamma_{s1}))\Big)\Bigg\}.\end{aligned} \tag{23}$$

$$\begin{aligned}\mathcal{U}_{cr}(R_s,\hat{s})\cap\mathcal{V}_2\cap\mathcal{B} = \Bigg\{&\boldsymbol{\gamma}_s\in\mathcal{Q}:(\eta_1(\gamma_{s1})\le\gamma_{s2}\le\gamma_{s1})\\ &\bigcap\Big((0<\gamma_{s1}<z_{b1}\cap 0\le\gamma_{s2}\le\gamma_{s1})\cup(z_{b1}<\gamma_{s1}<z_{b2}\cap 0\le\gamma_{s2}<\eta_{b2}(\gamma_{s1}))\Big)\\ &\bigcap\Big(\mathcal{P}_{pu}<\hat{s}\cap\gamma_{s1}>0\cap\eta_{b3}(\gamma_{s1})<\gamma_{s2}\le\gamma_{s1}\Big)\Bigg\}.\end{aligned} \tag{24}$$

$$\begin{aligned}\mathcal{U}_{cr}(R_s,\hat{s})\cap\mathcal{V}_2\cap\mathcal{C} = \Bigg\{&\boldsymbol{\gamma}_s\in\mathcal{Q}:(\eta_1(\gamma_{s1})\le\gamma_{s2}\le\gamma_{s1})\\ &\bigcap\Big((0<\gamma_{s1}<z_{c1}\cap 0\le\gamma_{s2}\le\gamma_{s1})\cup(z_{c1}<\gamma_{s1}<z_{c2}\cap 0\le\gamma_{s2}<\eta_{c2}(\gamma_{s1}))\Big)\\ &\bigcap\Big((\hat{s}\le\mathcal{P}_{pu}\cap\gamma_{s1}>0\cap 0<\gamma_{s2}<\eta_{a3}(\gamma_{s1}))\cup(\hat{s}>\mathcal{P}_{pu}\cap\gamma_{s1}>0\cap 0<\gamma_{s2}\le\eta_{b3}(\gamma_{s1}))\Big)\Bigg\}.\end{aligned} \tag{25}$$

All parameters appeared in (23), (24), and (25) are listed in table II.

In order to further illustrate the contribution of the regions $\mathcal{A}$, $\mathcal{B}$, and $\mathcal{C}$, we show these regions in Fig. 2. We note that the regions $\mathcal{A}$ and $\mathcal{B}$ do not appear in one figure, i.e., for one value

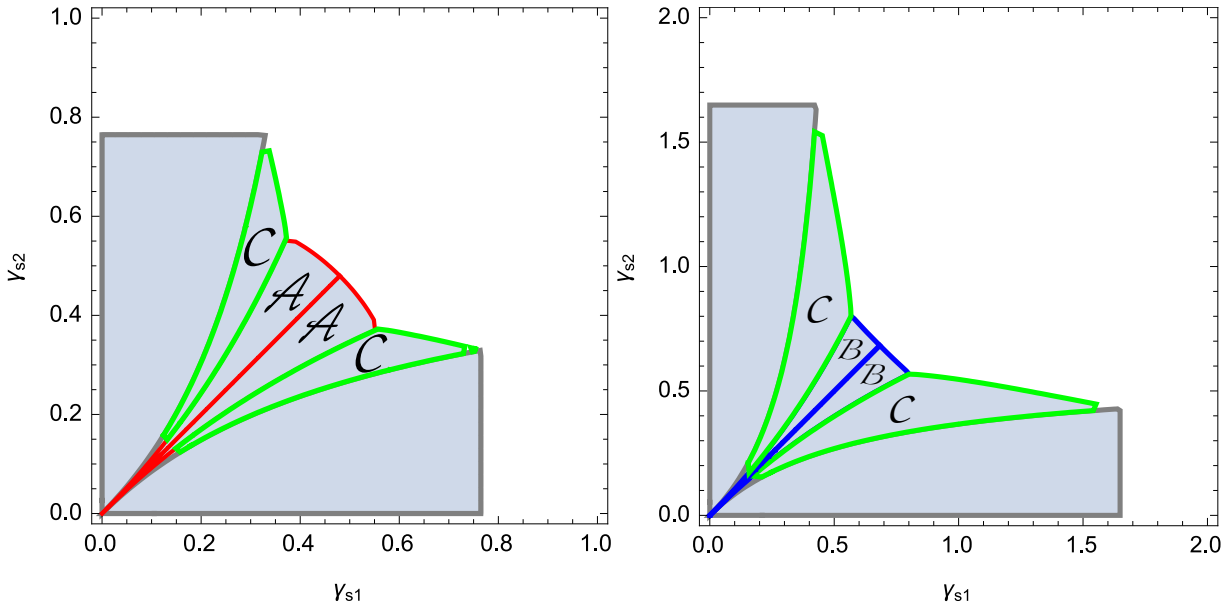

(a) The effect of regions $\mathcal{A}$ and $\mathcal{C}$ the on outage region at $\epsilon = 0.5$.

(b) The effect of regions $\mathcal{B}$ and $\mathcal{C}$ on the outage region at $\epsilon = 0.3$.

Fig. 2: Shapes and effects of the outage sub-regions ($\mathcal{A}$, $\mathcal{B}$, and $\mathcal{C}$) for different $\mathcal{P}_{pu}$ associated with $\epsilon = 0.5$ and $\epsilon = 0.3$.

$$
\begin{array}{lll}
\text{For } \gamma_{s1} \geq \gamma_{s2} & & \\
\text{If } :\boldsymbol{\gamma}_s \in [[\mathcal{U}_{cr}(R_s,\hat{s})]^c \cap \mathcal{V}_1] \cap \ [\hat{s} < \frac{\mathcal{P}_{pu}}{2}]; & \text{then: } \hat{p}_{s1} = 2\hat{s} & \hat{p}_{s2} = 0 \\
\text{If } :\boldsymbol{\gamma}_s \in [[\mathcal{U}_{cr}(R_s,\hat{s})]^c \cap \mathcal{V}_1] \cap \ [\hat{s} \geq \frac{\mathcal{P}_{pu}}{2}]; & \text{then: } \hat{p}_{s1} = \mathcal{P}_{pu}, & \hat{p}_{s2} = 0 \\
\text{If } :\boldsymbol{\gamma}_s \in [\mathcal{U}_{cr}(R_s,\hat{s}) \cap \mathcal{V}_1]\,; & \text{then: } \hat{p}_{s1} = 0, & \hat{p}_{s2} = 0 \\
\text{If } :\boldsymbol{\gamma}_s \in [[\mathcal{U}_{cr}(R_s,\hat{s})]^c \cap \mathcal{V}_2 \cap \mathcal{A}]\,; & \text{then: } \hat{p}_{s1} = \lambda_2 - \frac{1+\mathcal{P}_p\sigma_{ps}^2}{\gamma_{s1}}, & \hat{p}_{s2} = \lambda_2 - \frac{1+\mathcal{P}_p\sigma_{ps}^2}{\gamma_{s2}} \\
\text{If } :\boldsymbol{\gamma}_s \in [\mathcal{U}_{cr}(R_s,\hat{s}) \cap \mathcal{V}_2 \cap \mathcal{A}]\,; & \text{then: } \hat{p}_{s1} = 0, & \hat{p}_{s2} = 0 \\
\text{If } :\boldsymbol{\gamma}_s \in [[\mathcal{U}_{cr}(R_s,\hat{s})]^c \cap \mathcal{V}_2 \cap \mathcal{B}]\,; & \text{then: } \hat{p}_{s1} = \mathcal{P}_{pu}, & \hat{p}_{s2} = \mathcal{P}_{pu} \\
\text{If } :\boldsymbol{\gamma}_s \in [\mathcal{U}_{cr}(R_s,\hat{s}) \cap \mathcal{V}_2 \cap \mathcal{B}]\,; & \text{then: } \hat{p}_{s1} = 0, & \hat{p}_{s2} = 0 \\
\text{If } :\boldsymbol{\gamma}_s \in [[\mathcal{U}_{cr}(R_s,\hat{s})]^c \cap \mathcal{V}_2 \cap \mathcal{C}]\,; & \text{then: } \hat{p}_{s1} = \mathcal{P}_{pu}, & \hat{p}_{s2} = \lambda_2 - \frac{1+\mathcal{P}_p\sigma_{ps}^2}{\gamma_{s2}} \\
\text{If } :\boldsymbol{\gamma}_s \in [\mathcal{U}_{cr}(R_s,\hat{s}) \cap \mathcal{V}_2 \cap \mathcal{C}]\,; & \text{then: } \hat{p}_{s1} = 0, & \hat{p}_{s2} = 0
\end{array}
\quad . \tag{26}
$$

of $\mathcal{P}_{pu}$ either $\mathcal{A}$ or $\mathcal{B}$, but not both of them, appears in the outage region. This is because the intersection between these two regions is empty for a fixed $\mathcal{P}_{pu}$ for all values of γ_{s1} and γ_{s2}. To verify this, we expand both regions in Appendix A.

In **Step 3**, we derive the optimal power allocations, $\hat{p}_{s1}$ and $\hat{p}_{s2}$, which are expressed in (26). Note that the event $[\mathcal{U}]^c$ is the complement of the event $\mathcal{U}$ and $\lambda_2 = \frac{1+\mathcal{P}_p\sigma_{ps}^2}{2}\frac{\gamma_{s1}+\gamma_{s2}}{\gamma_{s1}\gamma_{s2}} + \hat{s}$. The symmetry between the power allocation under both cases of $\gamma_{s1} \leq \gamma_{s2}$ and $\gamma_{s1} \geq \gamma_{s2}$ is clear. Therefore, to extend the above results to the case where $\gamma_{s1} \leq \gamma_{s2}$, it suffices to swap the indices

in (21)-(26). The expressions in (26) are obtained by using the definitions of the sub-regions $\mathcal{A}$, $\mathcal{B}$, and $\mathcal{C}$ while substituting in (15). Note that, the optimal power of the first block is equivalent to $\frac{1+\mathcal{P}_p\sigma_{ps}^2}{2}\frac{\gamma_{s1}+\gamma_{s2}}{\gamma_{s1}\gamma_{s2}} + \hat{s} - \frac{1+\mathcal{P}_p\sigma_{ps}^2}{\gamma_{s1}}$, or $2\hat{s}$, or $\mathcal{P}_{pu}$, or 0, whereas the optimal power of the second block is expressed as $\frac{1+\mathcal{P}_p\sigma_{ps}^2}{2}\frac{\gamma_{s1}+\gamma_{s2}}{\gamma_{s1}\gamma_{s2}} + \hat{s} - \frac{1+\mathcal{P}_p\sigma_{ps}^2}{\gamma_{s2}}$, or $\mathcal{P}_{pu}$, or 0. This variation of expressions depends on the intersection of the outage/non-outage regions with the sub-region $\mathcal{V}_\mu$ (defined in the previous section) and the previously defined sub-regions $\mathcal{A}$, $\mathcal{B}$, and $\mathcal{C}$.

From the above analysis, it is clear that the optimal power profile together with the outage regions are tedious to derive, even for $M = 2$. Therefore, in the next section, we provide sub-optimal power strategies and their corresponding compact expressions of the outage probability. The associated outage probabilities of these strategies are shown to be lower and upper bounds on P_{out}^{+}. These bounds are shown to be optimal in a diversity order sense.

V. Sub-Optimal Strategies and Diversity Analysis

From the above section, it is clear that the optimal power profile, which achieves P_{out}^{+}, is cumbersome and difficult to compute. It is therefore of interest to provide simpler power allocation strategies with relevantly good outage performance. Hence, in the first sub-section below, we derive sub-optimal power strategies and the associated outage probabilities. In the second sub-section, we provide a diversity order analysis of the CR system.

A. Sub-Optimal Strategies

The first sub-optimal strategy consists of communication over a single channel block (selection-combining). In this strategy, the power allocated for the entire frame is transmitted in the block with the highest channel gain.

lemma 1. *The expression of the upper bound on the outage probability is obtained as follows,*

$$P_{out}^{u} = \left[F_{\gamma_s}\left(\frac{(e^{2MR_s}-1)(1+\mathcal{P}_p\sigma_{ps}^2)}{M\mathcal{P}_{bd}}\right)\right]^{M}, \tag{27}$$

where F_{γ_s} is the CDF of γ_{si} (since the elements of $\boldsymbol{\gamma}_s$ are independent and identicaly distributed

(i.i.d.)) and $\mathcal{P}_{bd}$ is defined as follows,

$$\mathcal{P}_{bd} = \min\left(\mathcal{P}^{st}, s^*, \mathcal{P}_{pu}\right). \tag{28}$$

Proof: The proof of Lemma is provided in Appendix B ■

It is clear that P_{out}^{u} decreases with $\mathcal{P}_{bd}$ and increases with R_s. It is also noted from [24] that the selection power policy is optimal in the low power regime.

The second sub-optimal strategy distributes the transmission power uniformly over all blocks. It is found that this strategy is optimal in the high power regime, i.e., $\mathcal{P}_{bd} \to \infty$, as stated in the following corollary.

lemma 2. *In high power regime, i.e., $\mathcal{P}_{bd} \to \infty$, the optimal power allocation of problem $\mathfrak{P}_1$ is to uniformly distribute the power over all available M blocks.*

Proof: The detailed proof is given in Appendix C. ■

Considering the optimal power allocation in the high power regime, i.e., $\mathcal{P}_{bd} \to \infty$, the associated asymptotic lower bound on the outage probability is derived in the following lemma.

lemma 3. *Utilizing the optimal power allocation in the high power regime, the associated asymptotic lower bound on the outage probability is derived as follows,*

$$P_{out}^{l,\infty} = \lim_{\mathcal{P}_{bd}\to\infty} F_U\left[\frac{M\left(e^{(2R_s)}-1\right)\left(1+\mathcal{P}_p\sigma_{ps}^2\right)}{\mathcal{P}_{bd}}\right], \tag{29}$$

where $F_U = F_{\sum_{i=1}^{M}\gamma_{si}}$ is the the CDF of the variable $U = \sum_{i=1}^{M}\gamma_{si}$, i.e., the sum of the SU channel gains over M blocks.

Proof: The detailed proof of Lemma 3 is given in Appendix D. ■

B. Diversity Analysis

In this sub-section, we investigate the diversity order of the proposed system in problem $\mathfrak{P}_1$. We begin by investigating the effect of the system's constraints on the budget power. The sub-optimal strategies, proposed in the previous section, are then utilized to derive the diversity order of the proposed system. In this sub-section, it is assumed that all the channel gains, i.e., $\boldsymbol{\gamma}_s$ and

γ_{ps}, follow an exponential distribution.

To analyze the diversity order performance, we study the impact of the system constraints on the budget power of SU as defined in (28). It is known that the diversity analysis is performed at budget power approaches infinity, $\mathcal{P}_{bd} \to \infty$. Thus, hereafter, we investigate each of the effective parameters on $\mathcal{P}_{bd}$, since the power budget $\mathcal{P}_{bd} \to \infty$ iff all the elements $\mathcal{P}^{st}$, s^*, and $\mathcal{P}_{pu}$ approach infinity. On the other hand, if one constraint approaches infinity while one or both others are finite constants, then this constraint becomes inactive. First, obviously, $\mathcal{P}^{st}$ directly affects $\mathcal{P}_{bd}$, with no dependence on other system parameters, i.e., if $\mathcal{P}^{st}$ is the only active constraint, then increasing $\mathcal{P}^{st}$ increases the budget power. Second, we observe that $\mathcal{P}_{pu} \to \infty$ when $\epsilon \to 1$: PU has a high tolerance for SU interference, $R_p \to 0$: PU is operating under a very low-rate constraint, and $\mathcal{P}_p \to \infty$: PU has a high power budget. Third, we consider the dependence between s^* and $\mathcal{P}^{lt}$ as observed in (18). This dependence is summarized in the following corollary.

Corollary 1. *The threshold s^* is related to $\mathcal{P}^{lt}$ as follows,*

$$\mathcal{P}^{lt} \to \infty \iff s^* \to \infty. \tag{30}$$

Proof: The proof is given in Appendix E. ■

Utilizing the upper bound and the asymptotic lower bound derived in (27) and (29), respectively, and considering the effect of the system parameters on $\mathcal{P}_{bd}$, the diversity order analysis is summarized in the following corollary.

Corollary 2. *The diversity order of the SU's outage probability is obtained as $d_{out} = -\lim_{\mathcal{P}_{bd}\to\infty} \frac{\log(P_{out})}{\log(\mathcal{P}_{bd})} = M$.*

Proof: A sketch of the SU's diversity order, d_{out}, proof is given as follows. We begin by investigating the corresponding diversity order of P_{out}^{+}. This is done by analyzing the diversity order of the upper and lower bounds of P_{out}^{+}, consequently, by considering the sub-optimal strategies proposed in the previous sub-section. Then, we compare the obtained diversity order of P_{out}^{+} with the diversity order of a similar system but without interference from PU, i.e.,

the lower bound on the exact outage probability, not P_{out}^{+}. This comparison leads to the exact diversity order of the system. The detailed proof is mentioned in Appendix F.

■

VI. Outage Analysis While Sensing Generalized PU Activity

In this section, SU's outage probability minimization problem is addressed while considering the generalized PU's activity via sensing information. Highlighting the sensing information impact on the system performance is an essential step since we are tackling a CR environment and the sensing step is necessary to realize the CR concept. The proposed formulation, in this section, combines both opportunistic and underlaying sharing approaches. Similar to previous sections, we begin by formulating the outage probability minimization problem. An AO algorithm is then proposed to obtain the optimal power allocation and the corresponding Lagrangian multipliers. We then prove the optimality of this algorithm. The minimum outage region under the sensing assumption is then derived.

The formulation of the problem, that consider the impact of sensing, depends on the generalized activity of PU. Accordingly, SU's mutual information is equal to $\mathcal{I}_M^{(0)}\left(\mathbf{p}_s\left(\boldsymbol{\gamma}_s\right)\right)$ if PU is idle and equal to $\mathcal{I}_M^{(1)}\left(\mathbf{p}_s\left(\boldsymbol{\gamma}_s\right)\right)$ if PU is active (both $\mathcal{I}_M^{(0)}$ and $\mathcal{I}_M^{(1)}$ are defined after the problem formulation). The probability of PU being active is captured by α_1, whereas the probability that the PU is idle is captured by $\alpha_0 = 1 - \alpha_1$. We assume that the errorness probabilities, i.e., miss-detection and false alarm probabilities, approach zeros due to employing an efficient sensing scheme, which also accounts for the sensing synchronization issues. We also note that the decision of the SU sensor about PU activity considers all the transmission blocks (in case the block-fading channels are separated by frequency not time), i.e., sensing all the blocks and comparing the resulting test statistic to a certain threshold and then making a decision. In the other case, where the block-fading channels are separated by time slots, the decision is made on the first block. This assumption is valid, and does not change the analysis, since PU's system is assumed to communicate over all M-blocks at each transmission time. The formulation of the problem is described as follows,

$$\mathfrak{P}_2: \quad \min_{\mathbf{p}_s(\boldsymbol{\gamma}_s)} \alpha_1 \Pr\left[\mathcal{I}_M^{(1)}\left(\mathbf{p}_s\left(\boldsymbol{\gamma}_s\right)\right) < R_s\right] + \alpha_0 \Pr\left[\mathcal{I}_M^{(0)}\left(\mathbf{p}_s\left(\boldsymbol{\gamma}_s\right)\right) < R_s\right] \tag{31a}$$

$$\text{s.t. } \mathfrak{F}_1: \ \langle \mathbf{p}_s\left(\boldsymbol{\gamma}_s\right)\rangle \leq \mathcal{P}^{st} \tag{31b}$$

$$\mathfrak{F}_2: \ \mathbb{E}\{\langle \mathbf{p}_s(\boldsymbol{\gamma}_s)\rangle\} \leq \mathcal{P}^{lt} \tag{31c}$$

$$\mathfrak{F}_{3i}: \ \Pr\left[\mathcal{I}_i^{(p-)} < R_p \middle| \gamma_{si}\right] \leq \epsilon, \ \forall\, i \in \{1, ..., M\}. \tag{31d}$$

where $\mathcal{I}_M^{(1)}(\mathbf{p}_s(\boldsymbol{\gamma}_s)) = \frac{T_c}{2MT}\sum_{i=1}^{M}\log\left(1+\frac{p_i(\boldsymbol{\gamma}_s)\gamma_{si}}{1+\mathcal{P}_p\sigma_{ps}^2}\right)$ is the SU's mutual information when PU is active. Hence, $\mathcal{I}_M^{(0)}(\mathbf{p}_s(\boldsymbol{\gamma}_s)) = \frac{T_c}{2MT}\sum_{i=1}^{M}\log\left(1+p_{si}(\boldsymbol{\gamma}_s)\gamma_{si}\right)$ is the SU's mutual information when PU is idle. The parameters T_s and T_c are the sensing and communication time of the SU, respectively, such that $T = T_c + T_s$. PU's mutual information, per block, $\mathcal{I}_i^{(p-)}$, is defined similarly to PU's mutual information in (13d). Similar to constraint (13d), constraint $\mathfrak{F}_{3i}$ is reduced to $p_{si}(\gamma_{si}) \leq \left[\frac{F_{\gamma_p}^{-1}(\epsilon)\mathcal{P}_p}{(e^{2R_p}-1)\sigma_{sp}^2} - \frac{1}{\sigma_{sp}^2}\right]_0 = \mathcal{P}_{pu}$.

Problem $\mathfrak{P}_2$ is difficult to solve using conventional techniques. This is due to the fact that the objective function is a weighted sum of non-convex and non-linear functions, i.e., a weighted sum of the outage probabilities. Therefore, to obtain the minimum outage region, we propose an algorithm that utilizes the structure of problem $\mathfrak{P}_2$ with respect to (w.r.t.) each optimization variable. The optimization variables are the allocated power policies. These variables are divided into two power policies, based on the sensed activities of PU, i.e., active and idle. The optimal power policy is summarized in the following theorem.

Theorem 4. *The optimal power allocation that solves problem $\mathfrak{P}_2$ is obtained as follows,*

$$p_{si}(\gamma_s) = \begin{cases} p_{ni}(\gamma_s) & ;\boldsymbol{\gamma}_s \notin [\mathcal{U}_{cr} \ \cap \ \textit{PU is ON}] \\ p_{fi}(\gamma_s) & ;\boldsymbol{\gamma}_s \notin [\mathcal{U}_{cr} \ \cap \ \textit{PU is OFF}] \\ 0 & ;\boldsymbol{\gamma}_s \in [\mathcal{U}_{cr} \ \cap \ [\textit{PU is OFF} \cup \textit{PU is ON}]] \end{cases}, \tag{32}$$

where the power profiles are defined as follows, $p_{fi}(\gamma_s) = \min\left(\frac{T_c\lambda_f^{(q)}(\mu_f,\boldsymbol{\gamma}_s)}{T} - \frac{1}{\gamma_{si}}, \ \mathcal{P}_{pu}\right)$ *and* $p_{ni}(\gamma_s) = \min\left(\frac{T_c\lambda_n^{(q)}(\mu_n,\boldsymbol{\gamma}_s)}{T} - \frac{1+\mathcal{P}_p\sigma_{ps}^2}{\gamma_{si}}, \ \mathcal{P}_{pu}\right)$*. The associated parameters* $\lambda_f^{(q)}(\mu_f,\boldsymbol{\gamma}_s)$ *and* $\lambda_n^{(q)}(\mu_n, \boldsymbol{\gamma}_s)$ *are obtained from the output of the proposed Algorithm 1. The following definitions are used in Algorithm 1,*

$$\lambda_f^{(q)}(\mu_f,\boldsymbol{\gamma}_s) = \frac{T}{T_c\mu_f}\sum_{l=1}^{\mu_f}\frac{1}{\gamma_{sl}} + \frac{TM}{T_c\mu_f}\hat{s}_f^{(q)} \quad \textit{and} \quad p_{fi}^{(q)} = \min\left(\frac{T_c\lambda_f^{(q)}(\mu_f,\boldsymbol{\gamma}_s)}{T} - \frac{1}{\gamma_{si}}, \ \mathcal{P}_{pu}\right), \tag{33}$$

$$\lambda_n^{(q)}(\mu_n, \boldsymbol{\gamma}_s) = \frac{T(1+\mathcal{P}_p\sigma_{ps}^2)}{T_c\mu_n}\sum_{l=1}^{\mu_n}\frac{1}{\gamma_{sl}} + \frac{TM}{T_c\mu_n}\hat{s}_n^{(q)} \quad \textit{and} \quad p_{ni}^{(q)} = \min\left(\frac{T_c\lambda_n^{(q)}(\mu_n,\boldsymbol{\gamma}_s)}{T} - \frac{1+\mathcal{P}_p\sigma_{ps}^2}{\gamma_{si}},\ \mathcal{P}_{pu}\right). \tag{34}$$

The superscript (q) designates the iteration number in Algorithm 1. Note that

$$\hat{s}_f^{(q)} = \min\left(\mathcal{P}^{st}, s_f^{(q)}\right) \textit{ and } \hat{s}_n^{(q)} = \min\left(\mathcal{P}^{st}, s_n^{(q)}\right). \tag{35}$$

The parameters $s_n^{(q)}$ and $s_f^{(q)}$ are obtained by solving,

$$\alpha_1 \int_{\overline{\mathcal{R}_{cr}}(s_n^{(q)})} \langle \mathbf{p}_n(\gamma_s)\rangle dG(\boldsymbol{\gamma}_s) + \alpha_0 \int_{\overline{\mathcal{R}_{cr}}(s_f^{(q)})} \langle \mathbf{p}_f(\gamma_s)\rangle dG(\boldsymbol{\gamma}_s) = \mathcal{P}^{lt}. \tag{36}$$

Algorithm 1: AO Algorithm

input : $\mathcal{P}^{st}$, $\mathcal{P}^{lt}$, α, γ_s, $\mathcal{P}_p\sigma_{ps}^2$, σ_{sp}^2, ϵ, $\hat{s}$, T, T_c

Initialize: $s_f^{(0)} = s_n^{(0)} = s^*$ which is obtained from (18), $\hat{s}_f^{(0)}$ and $\hat{s}_n^{(0)}$ are obtained from (35), $cond = True$;

$q = 1$

while *cond* **do**

  For a fixed $s_n^{(q-1)}$, Update $s_f^{(q)}$ from (36) and $\hat{s}_f^{(q)}$ from (35).

  Find $\lambda_f^{(q)}(\mu_f, \boldsymbol{\gamma}_s)$ and $p_{fi}^{(q)}$ as in (33), for a fixed $p_{ni}^{(q-1)}$ and $\lambda_n^{(q-1)}(\mu_n, \boldsymbol{\gamma}_s)$.

  For a fixed $s_f^{(q)}$, Update $s_n^{(q)}$ from (36) and $\hat{s}_n^{(q)}$ from (35).

  Find $\lambda_n^{(q)}(\mu_n, \boldsymbol{\gamma}_s)$ and $p_{fi}^{(q)}$ as in (34), for a fixed $p_{fi}^{(q)}$ and $\lambda_f^{(q)}(\mu_f, \boldsymbol{\gamma}_s)$.

  Find outage probability ($P_{out}^{(q)}$) by substituting in,

$$P_{out}^{(q)} = \alpha_1 \Pr\left[\mathcal{I}_M^{(1)}\left(\mathbf{p}_n^{(q)}\right) < R_s\right] + \alpha_0 \Pr\left[\mathcal{I}_M^{(0)}\left(\mathbf{p}_f^{(q)}\right) < R_s\right] \tag{37}$$

  if $\left\| P_{out}^{(q)} - P_{out}^{(q-1)} \right\| < \epsilon$ **then:** $cond = False$

  q = q+1;

end

output: $\lambda_f^{(q)}(\mu_f, \boldsymbol{\gamma}_s)$, $\lambda_n^{(q)}(\mu_n, \boldsymbol{\gamma}_s)$

Proof: Note that the objective function of problem $\mathfrak{P}_2$ is a weighted sum of two outage probabilities, i.e., $\Pr\left[\mathcal{I}_M^{(1)}\left(\mathbf{p}_n(\gamma_s)\right) < R_s\right]$ and $\Pr\left[\mathcal{I}_M^{(0)}\left(\mathbf{p}_f(\gamma_s)\right) < R_s\right]$. Therefore, if we fix one outage probability, say, the one associated with $\mathcal{I}_M^{(0)}$, then problem $\mathfrak{P}_2$ becomes equivalent to problem $\mathfrak{P}_1$. Similarly, if we fix the second outage probability term, which is associated with $\mathcal{I}_M^{(1)}$, then problem $\mathfrak{P}_2$ is solved in a similar way as $\mathfrak{P}_1$. Utilizing the previous discussion, we note that the best optimization tool to solve problem $\mathfrak{P}_2$ is the AO technique. This iterative algorithm guarantees a global solution for specific structures of the problem w.r.t. the optimization

variables. Under many of these structures, i.e., pseudo-convexity or strict quasi-convexity w.r.t. each optimization variable, the global optimality convergence of the AO algorithm is proven in [25], [26][Ch. 10]. Therefore, to utilize the AO algorithm in obtaining the optimal solution, it is necessary to prove the strict quasi-convexity structure of each of the outage probability terms w.r.t. each optimization variable. We first divide the power allocation variable $p_{si}\left(\gamma_s\right)$ into two variables depending on the activity of the PU, i.e., $p_{si}\left(\gamma_s\right) = p_{fi}\left(\gamma_s\right)$ when PU is idle, and $p_{si}\left(\gamma_s\right) = p_{ni}\left(\gamma_s\right)$ when PU is active. Second, we prove the strict quasi-convexity structure of the objective function w.r.t. each variable, $p_{ni}\left(\gamma_s\right)$ and $p_{fi}\left(\gamma_s\right)$. Let us begin by verifying the strict quasi-convexity of $\Pr\left[\mathcal{I}_M^{(0)}(\mathbf{p}_f\left(\gamma_s\right)) < R_s\right]$ w.r.t. $p_{fi}\left(\gamma_s\right)$. The other outage probability term can be analyzed in a similar way. A strictly quasi-convex function is defined as follows [27] (note that for the ease of notation, and generality of the proof, we let $f(\mathbf{x}) = \Pr\left[\mathcal{I}_M^{(0)}\left(\mathbf{x}\right) < R_s\right]$, where $\mathbf{x} = \mathbf{p}_f\left(\gamma_s\right)$),

Definition A function f defined on a convex set $S \subseteq \mathfrak{R}^n$ is said to be strictly quasi-convex if $f\left(\lambda\mathbf{x}_1 + (1-\lambda)\mathbf{x}_2\right) < \max\left\{f\left(\mathbf{x}_1\right), f\left(\mathbf{x}_2\right)\right\}$, for every $\mathbf{x}_1, \mathbf{x}_2 \in S,\ \ \mathbf{x}_1 \neq \mathbf{x}_2,\ \lambda \in (0,1)$.

It is known that the outage probability, $f(\mathbf{x})$, decreases by increasing the transmission power, i.e., $\mathbf{x}$. It follows that for $\mathbf{x}_1 < \mathbf{x}_2 \implies f(\mathbf{x}_1) \geq f(\mathbf{x}_2)$. Thus, to prove that $f(\mathbf{x})$ is strictly quasi-convex, we must verify that,

$$f\left(\lambda\mathbf{x}_1 + (1-\lambda)\mathbf{x}_2\right) < f\left(\mathbf{x}_1\right), \quad \text{if} : \mathbf{x}_1 < \mathbf{x}_2. \tag{38}$$

Recall that $f(\mathbf{x})$ represents an outage probability; hence, it is a multi-dimensional integration of a joint probability density function (PDF), of the channel $\boldsymbol{\gamma}_s$, over specific bounds, defined as,

$$f(\mathbf{x}) = \int_0^{\frac{T_c}{2MT}\sum_{i=1}^{M}\log(1+\gamma_{si}x_i)<R_s} \cdots \int f_{\boldsymbol{\gamma}_s}(\boldsymbol{\gamma}_s) \quad d\gamma_s. \tag{39}$$

where $f_{\boldsymbol{\gamma}_s}(\boldsymbol{\gamma}_s) = f_{\gamma_{s1}}(\gamma_{s1}) \ldots f_{\gamma_{sM}}(\gamma_{sM})$ and $d\boldsymbol{\gamma}_s = d\gamma_{s1} \ldots d\gamma_{sM}$. It is easy to see that the lower bound of each of the integrals is 0, whereas the upper bound of the multi-dimension integral is determined by the outage region, i.e., $\frac{T_c}{2MT}\sum_{i=1}^{M}\log\left(1+\gamma_{si}x_i\right) < R_s$. Substituting (39) into

(38), it follows that we need to verify the following,

$$\int_{0}^{\mathcal{O}_\lambda(\mathbf{x})} \cdots \int f_{\boldsymbol{\gamma}_s}(\boldsymbol{\gamma}_s) \quad d\boldsymbol{\gamma}_s < \int_{0}^{\mathcal{O}(\mathbf{x})} \cdots \int f_{\boldsymbol{\gamma}_s}(\boldsymbol{\gamma}_s) \quad d\boldsymbol{\gamma}_s, \tag{40}$$

where $\mathcal{O}_\lambda(\mathbf{x}) = \{\boldsymbol{\gamma}_s \in \mathbb{R}_+^M : \ \frac{T_c}{2MT}\sum_{i=1}^{M}\log\left(1+\gamma_{si}\left(\lambda x_{1i}+(1-\lambda)x_{2i}\right)\right) < R_s$ and $\mathcal{O}(\mathbf{x}) = \{\boldsymbol{\gamma}_s \in \mathbb{R}_+^M : \ \frac{T_c}{2MT}\sum_{i=1}^{M}\log\left(1+\gamma_{si}x_{1i}\right) < R_s\}$. Note that the integrand term is the PDF of the BF channels $\boldsymbol{\gamma}_s$, which is a non-negative quantity. The integral region is the only difference between the term before and after the inequality in (40). It follows that verifying (40) is equivalent to proving that $\mathcal{O}_\lambda \subset \mathcal{O}$, as proved in Appendix H. To verify that $\mathcal{O}_\lambda \subset \mathcal{O}$, it is necessary to show that,

$$\frac{T_c}{2MT}\sum_{i=1}^{M}\log\left(1+\gamma_{si}\left(\lambda x_{1i}+(1-\lambda)x_{2i}\right)\right) > \frac{T_c}{2MT}\sum_{i=1}^{M}\log\left(1+\gamma_{si}x_{1i}\right). \tag{41}$$

Knowing that $\frac{1}{2M}\sum_{i=1}^{M}\log\left(1+\gamma_{si}x_{1i}\right)$ is a strictly increasing concave function, it is therefore strictly quasi-concave. Furthermore, through our previous assumption, i.e., $\mathbf{x}_1 < \mathbf{x}_2$, and knowing that the sum of logarithms is an increasing function of $\mathbf{x}$, it follows that,

$$\min\left\{\frac{T_c}{2MT}\sum_{i=1}^{M}\log\left(1+\gamma_{si}x_{1i}\right), \frac{T_c}{2MT}\sum_{i=1}^{M}\log\left(1+\gamma_{si}x_{2i}\right)\right\} = \frac{T_c}{2MT}\sum_{i=1}^{M}\log\left(1+\gamma_{si}x_{1i}\right). \tag{42}$$

We again refer to the definition of the strictly quasi-concave function as follows.

Definition A function f defined on a convex set $S \subseteq \Re^n$ is said to be strictly quasi-concave if and only if $g\left(\lambda\mathbf{x}_1+(1-\lambda)\mathbf{x}_2\right) > \min\left\{g\left(\mathbf{x}_1\right), g\left(\mathbf{x}_2\right)\right\}$ for every $\mathbf{x}_1, \mathbf{x}_2 \in S, \ \ \mathbf{x}_1 \neq \mathbf{x}_2$, and for every $\lambda \in (0,1)$.

Let $g(\mathbf{x}) = \frac{T_c}{2MT}\sum_{i=1}^{M}\log\left(1+\gamma_{si}x_i\right)$. Utilizing the quasi-concavity of $g(\mathbf{x})$ and (42), we can easily prove (41) and (40). Therefore, we note that the outage probability $\Pr\left[\mathcal{I}_M^{(0)}\left(\mathbf{p}_f\left(\gamma_s\right)\right) < R_s\right]$ is strictly quasi-convex function. In similar steps to those in the above proof, we prove that $\Pr\left[\mathcal{I}_M^{(1)}\left(\mathbf{p}_n\left(\gamma_s\right)\right) < R_s\right]$ is a strictly quasi-convex function w.r.t. $\mathbf{p}_n\left(\gamma_s\right)$. This finalizes the proof of the optimality of the AO algorithm. Thus, the power allocation policy in (32) is an optimal policy.

■

The optimal power policy, derived in Theorem 4, is constructed of a piece-wise function,

which combines both opportunistic and underlaying sharing approaches. If the sensing scheme decide that PU is active then SU transmits with $p_{ni}\left(\gamma_s\right)$ power policy under no-outage. If the sensing scheme decide that PU is idle then SU transmits using $p_{fi}\left(\gamma_s\right)$ power policy under no-outage region. If there is an outage even under all cases of PU's activity then SU does not transmit.

The corresponding SU outage region, under sensing information, is defined as the union of the outage region intersections with all the positive power regions, i.e., $\left[\bigcup_{\mu_n=1}^{M} \mathcal{U}_{cr}(R_s, \hat{s}_n, \hat{s}_f) \bigcap \mathcal{V}_{\mu_n}\right] \cup \left[\bigcup_{\mu_f=1}^{M} \mathcal{U}_{cr}(R_s, \hat{s}_n, \hat{s}_f) \cap \mathcal{V}_{\mu_f}\right]$. The region $\mathcal{V}_{\mu_n}$ is a sub-region of $\mathcal{Q}$, defined such that the corresponding power elements of $\mathbf{p}_n\left(\gamma_s\right)$ are positive, i.e., $\left\{p_{ni}\left(\gamma_s\right), \ldots, \; p_{ni}\left(\gamma_s\right)\right\} \geq 0$. The integer μ_n is the unique number in $\{1, \ldots, M\}$, such that $\frac{T\left(1+\mathcal{P}_p\sigma_{ps}^2\right)}{T_c\gamma_{sm}} \leq \lambda_n^{(q)}$ for $m \leq \mu$ and $\frac{T\left(1+\mathcal{P}_p\sigma_{ps}^2\right)}{T_c\gamma_{sm}} > \lambda_n^{(q)}$ for $m > \mu_n$. Region $\mathcal{V}_{\mu_f}$ is defined similarly to $\mathcal{V}_{\mu_n}$, but associated with the positive power elements of $\mathbf{p}_f\left(\gamma_s\right)$. Each of the outage region intersections is defined as follows,

$$\mathcal{U}_{cr}(R_s, \hat{s}_n, \hat{s}_f) \cap \mathcal{V}_{\mu_f} = \left\{\boldsymbol{\gamma}_s \in \mathcal{Q} : \; \frac{\alpha_0 T_c}{2TM} \sum_{m=1}^{\mu_f} \log\left(1 + \gamma_{sm} p_{fi}\left(\gamma_s\right)\right) < R_s\right\}, \tag{43}$$

$$\mathcal{U}_{cr}(R_s, \hat{s}_n, \hat{s}_f) \cap \mathcal{V}_{\mu_n} = \left\{\boldsymbol{\gamma}_s \in \mathcal{Q} : \; \frac{\alpha_1 T_c}{2TM} \sum_{m=1}^{\mu_n} \log\left(1 + \frac{\gamma_{sm} p_{ni}\left(\gamma_s\right)}{1 + \mathcal{P}_p\sigma_{ps}^2}\right) < R_s\right\}, \tag{44}$$

where the Lagrangian multipliers $\lambda_n^{(q)}(\mu_n, \boldsymbol{\gamma}_s)$ and $\lambda_f^{(q)}(\mu_f, \boldsymbol{\gamma}_s)$ are obtained from the output of Algorithm 1. The effect of PU activity is noted through the influence of the probabilities α_1 and α_0 on the outage region. Furthermore, the sensing effect appears in the output of Algorithm 1, i.e., $\lambda_n^{(q)}(\mu_n, \boldsymbol{\gamma}_s)$ and $\lambda_f^{(q)}(\mu_f, \boldsymbol{\gamma}_s)$. It is also noted that $\mathcal{V}_{\mu_n}$ and $\mathcal{V}_{\mu_f}$ contribute differently to the minimum outage region.

VII. Numerical Evaluation

In this section, the outage probability of SU (P_{out}^{+}) over multiple blocks is evaluated. The outage region corresponding to the derived analytical expressions of communication over two blocks, $M = 2$, is shown. Finally, numerical analysis compares P_{out}^{+} to the upper and lower bounds formulas given by (27) and (29), respectively. Evaluation of the system with and without sensing information is also presented. We consider that all the channel gains, γ_{si}, γ_p, γ_{psi}, and

γ_{spi} follow an exponential distribution.

TABLE III: SIMULATION PARAMETERS.

Parameter Name	**Value**
Wireless channels	Rayleigh, Slow Flat Fading
# Coherence Blocks (M)	2
$\mathcal{P}_p$	10 dB
P^{st}	10 dB
P^{lt}	15 dB
ϵ	0.1
σ^2_{sp}, σ^2_{ps}	1

Fig. 3 shows the outage region, derived in (21) - (25) corresponding to $M = 2$. It is observed that the outage region decreases by increasing $\hat{s}$, in (4). The shape of the outage region changes based on the relationship between $\hat{s}$ and $\mathcal{P}_{pu}$. To further illustrate this point, when $\hat{s} = 8$ dB, the CR constraint is not active because $\hat{s} < \frac{\mathcal{P}_{pu}}{2}$. The shape of the outage region (a) is similar to that in [5]. When $\hat{s}$ increases to $\hat{s} = 10$ dB or 12 dB, it is clear that $\mathcal{P}_{pu} > \hat{s} > \frac{\mathcal{P}_{pu}}{2}$. We note that unlike the region in (a), the corresponding outage regions, (b) and (c), are not convex. Increasing $\hat{s}$ to 16 dB, where $\hat{s} > \mathcal{P}_{pu}$, results in a partial alignment in the outage region (d) with region (e). Finally, we observe that increasing $\hat{s}$ to a relatively large value (w.r.t. $\mathcal{P}_{pu}$) does not change the outage region's shape, as in (e). This saturation (fixed shape) of the outage region occurs because $\hat{s}$ is relatively high and the active budget power becomes $\mathcal{P}_{pu}$ for all realizations of the two-block channel.

Fig. 4 shows the outage probability performance versus the PU rate, R_p, for different numbers of fading blocks, $M = 2$, $M = 3$, and different values of ϵ. Fig. 4 shows that the outage probability increases with increasing R_p. In addition, Fig. 4 shows that the outage performance is saturated at $P_{out} = 0.0025$ for $R_p \leq 0.01$, $R_p \leq 0.1$, and $R_p \leq 0.2$ for $M = 2$ and $\epsilon = 0.4$, $\epsilon = 0.6$, and $\epsilon = 0.8$, respectively. On the other hand, the outage probability is saturated at $P_{out} = 0.000173$ for $R_p \leq 0.01$, $R_p \leq 0.07$, and $R_p \leq 0.12$ for $M = 3$ and $\epsilon = 0.4$, $\epsilon = 0.6$, and $\epsilon = 0.8$, respectively. This saturation region occurs because of the cognitive constraint becomes an inactive constraint when R_p is relatively small and becomes active when R_p is relatively large or ϵ gets smaller. Increasing the number of fading blocks, M, decreases the outage probability. This observation supports the claim that by decoding over

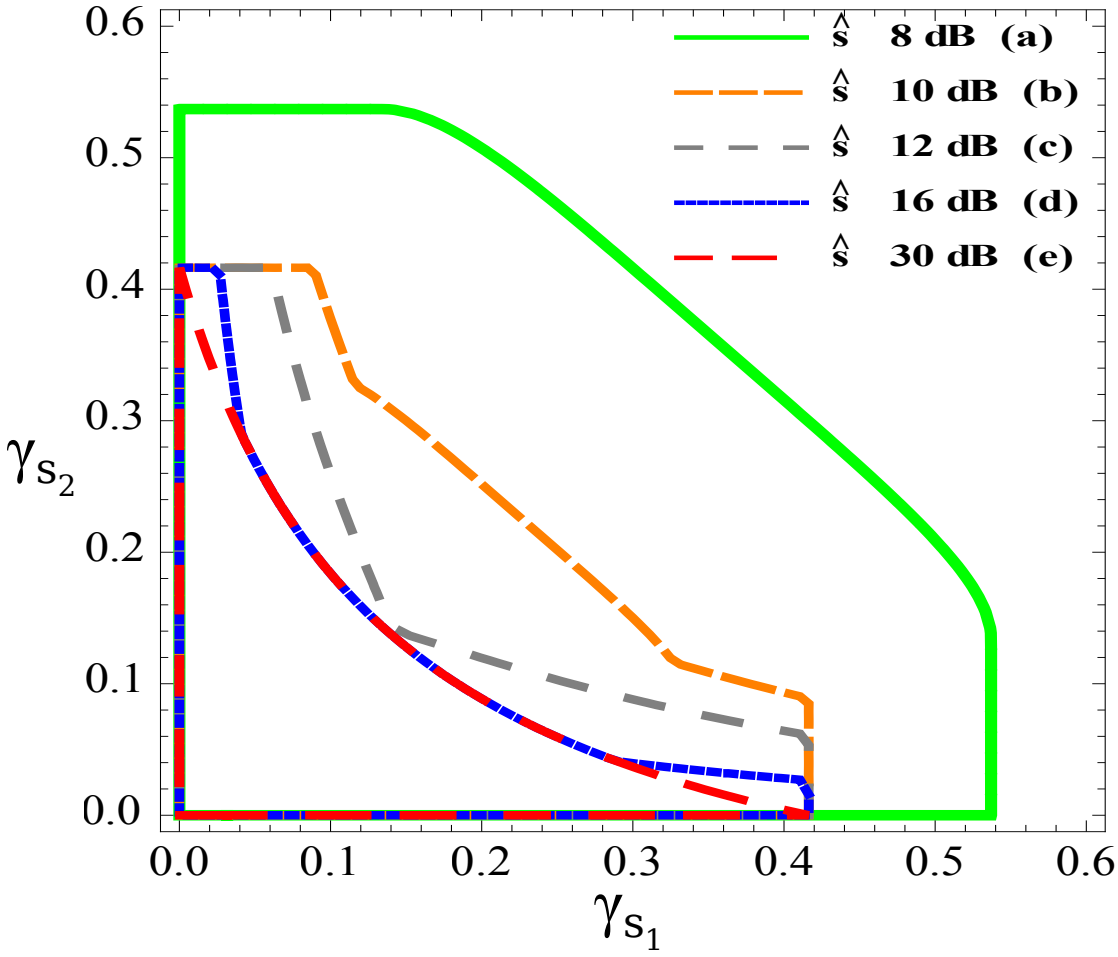

Fig. 3: Outage region for different $\hat{s}$, $M = 2$, and $\mathcal{P}_{pu} = 12.1$ dB.

multiple blocks, the system's robustness increases with the same Signal-to-Interference-Noise-Ratio (SINR). Therefore, in practical implementations, it is necessary to consider the trade-off between increasing the number of blocks (which works better at low SINR) and decreasing the delay (at high SINR).

Fig. 5 shows a comparison among the upper bound (P_{out}^{u}), lower bound (P_{l}), and asymptotically lower bound ($P_{out}^{l,\infty}$) w.r.t. P_{out}^{+} for $M = 2$. It is observed that the slope of P_{out}^{+}, P_{out}^{u}, P_{out}^{l}, and $P_{out}^{l,\infty}$ is equal to 2. This supports the results in Corollary 2. We note that the difference between P_{out}^{+} and P_{out}^{u}, P_{out}^{+} and P_{out}^{l} is similar, i.e., about 2 dB at high SINR. It is observed that $P_{out}^{l,\infty}$ achieves a tighter bound to P_{out}^{+} at high SINR in comparison with P_{out}^{l}.

Fig. 6 shows the outage probability of the SU with sensing information versus the SU rate threshold, R_s, for different α_1. This figure shows that the system with sensing information

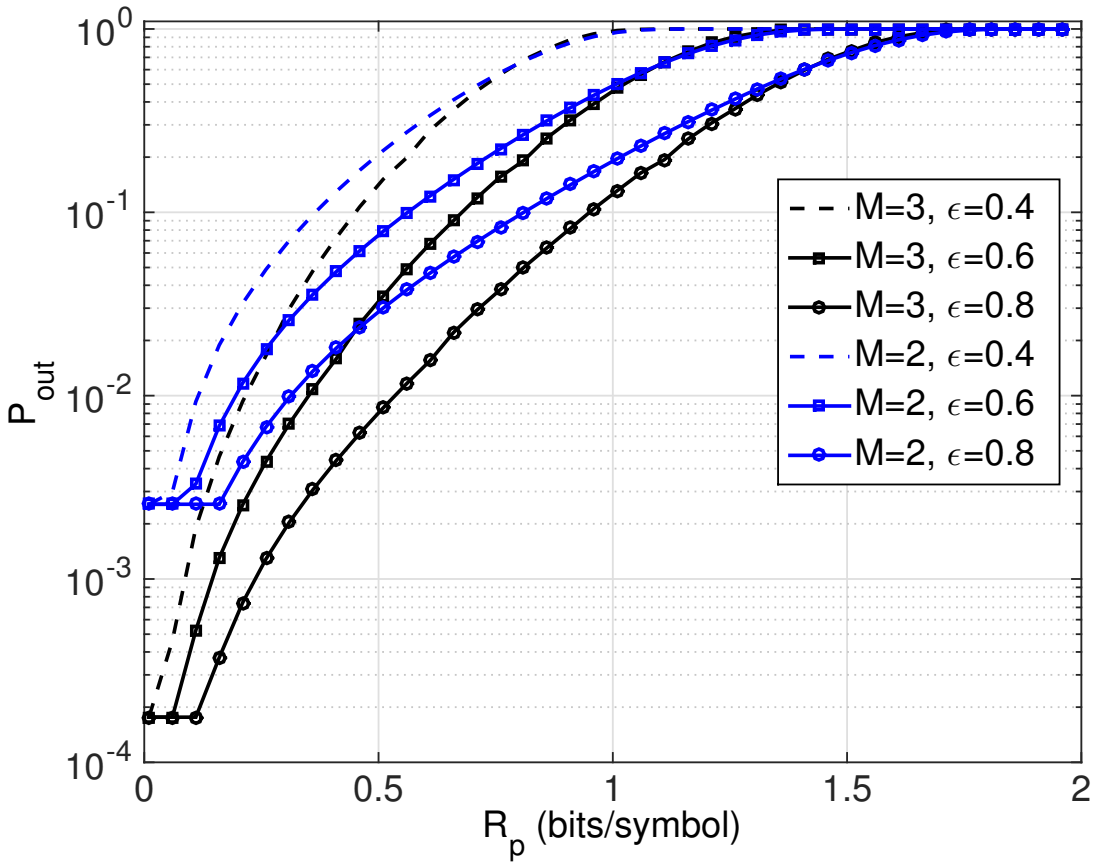

Fig. 4: P_{out} performance with varying R_p for different $M = 2, 3$ and $\epsilon = 0.4, 0.6, 0.8$.

and $\alpha_1 \to 1$ performs similarly to the system without sensing information while having PU interference, indicated in Fig. 6 as "No PU". Likewise, as $\alpha_1 \to 0$, the system with sensing information performs similarly to the one without PU interference, indicated as "PU". This is expected since both cases of $\alpha_1 \to 1$ and $\alpha_1 \to 0$ are the performance limits of the system with sensing information. We also note that decreasing α_1 results in degradation of the system performance. Obviously, increasing SU's minimum rate, R_s, results in increasing the outage probability.

In addition to evaluating our underlaying proposed scheme versus [5]'s scheme (as shown in Fig. 3), we consider another scheme from the state-of-the-art, i.e., opportunistic spectrum sharing [7], [6], [9]. This scheme enables SU to transmit on the un-utilized licensed spectrum bands of PU after sensing the spectrum. If the PU is active then SU cannot transmit. In the following two figures, this scheme is denoted as "OS". Whereas, our first proposed scheme, in Sec. III,

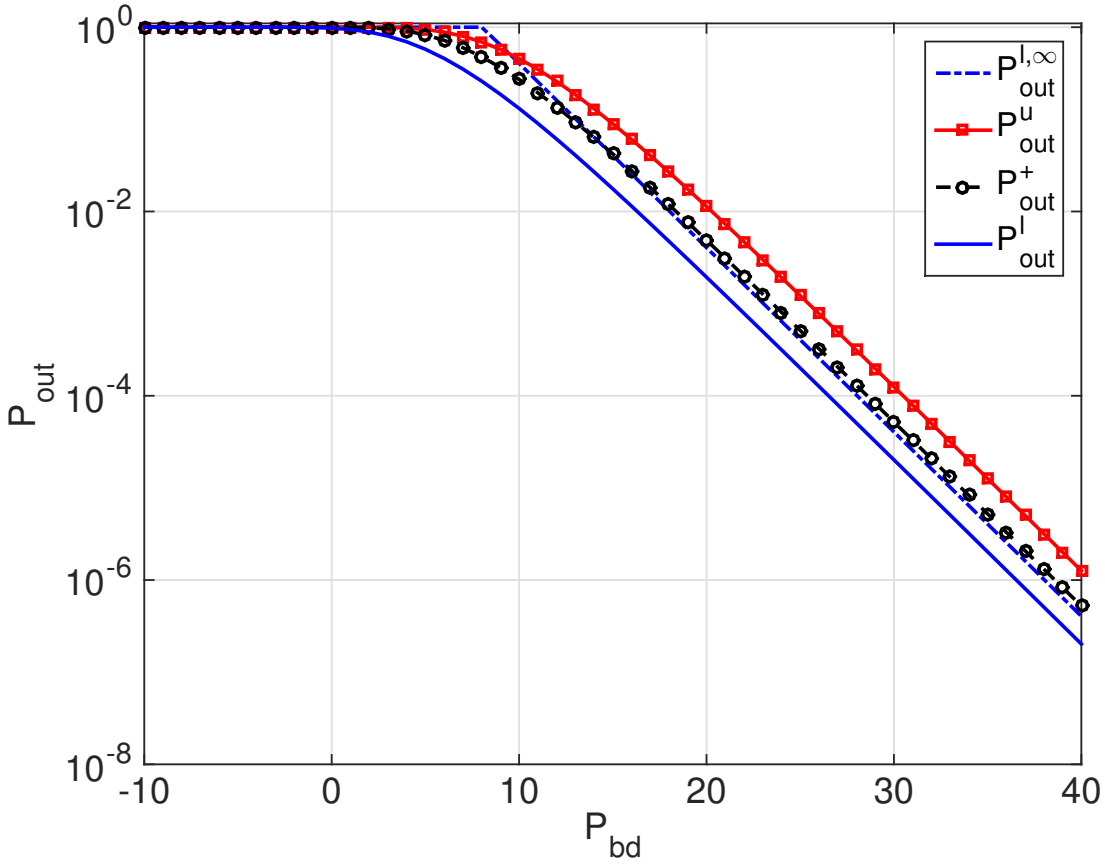

Fig. 5: Comparing the lower and upper bounds with the exact numerical results for $M = 2$.

i.e., underlaying sharing, is denoted as "US". The proposed combined sensing and underlaying scheme, in Sec. VI, is denoted as "WSNS".

Fig. 7 shows the outage probability of all three schemes versus the primary transmission power, $\mathcal{P}_p$, and primary generalized activity probability, α_1. Several observations are made from Fig. 7. It is noted that for any value of α_1 the proposed combined scheme "WSNS" outperforms the other schemes "US" and "OS". The increase of $\mathcal{P}_p$ leads to an inactive PU's interference constraint. Therefore, we notice the saturation of all scheme's outage probability with the increase of $\mathcal{P}_p$. We note that this saturation continues up to $\mathcal{P}_p = 35$ dB and further for "OS", however, for both schemes "US" and "WSNS", the P_{out} start increasing again for high $\mathcal{P}_p$. The reason behind this phenomena is that, even if the PU's interference constraint is inactive, the interference from PU to SU increases with $\mathcal{P}_p$. Since both "WSNS" and "US" outage performance depends on the interference form PU to SU, thus, increasing the interference leads to increase the outage

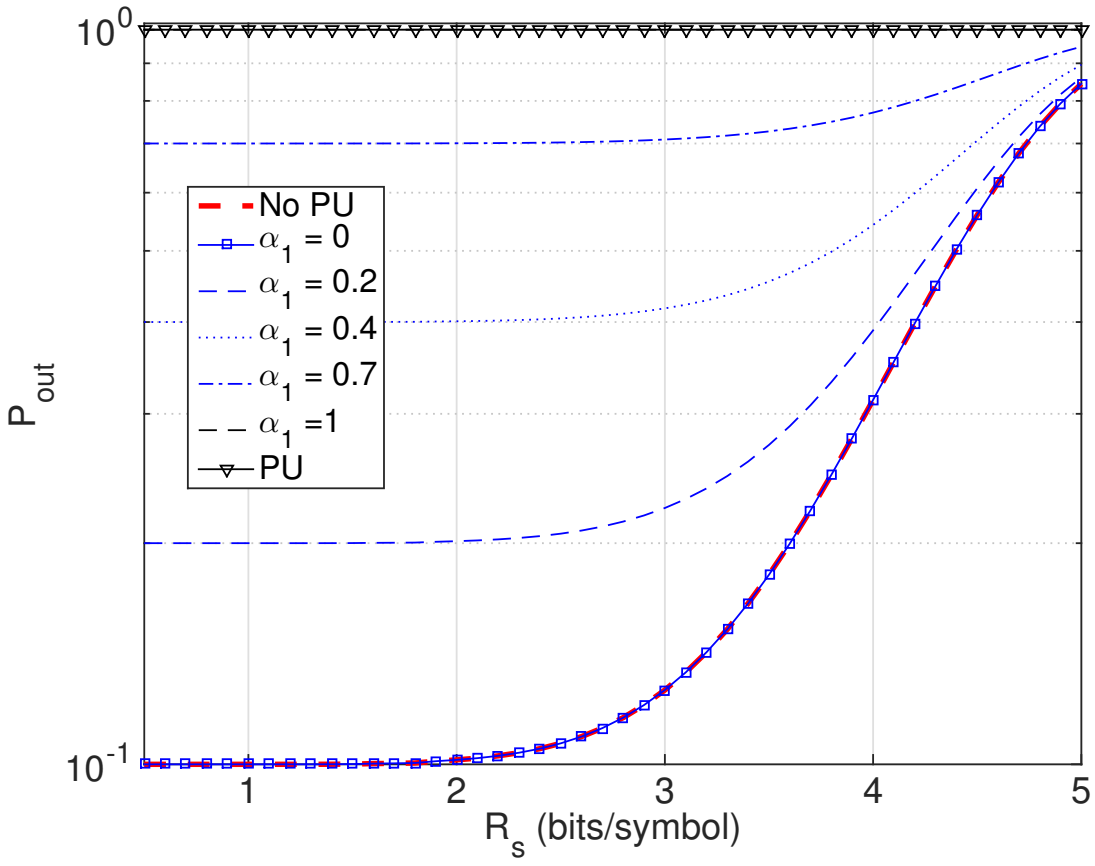

Fig. 6: The outage probability of the SU system with sensing information versus R_s, for different α_1, and $\epsilon = 0.5$.

probability of both schemes. However, since "OS" does not depend on the interference, because it transmit only when PU is idle, the outage probability of this scheme remains without changes as $\mathcal{P}_p \to \infty$. It is also observed that changing α_1 does not change the outage performance of "US". That is expected from our analysis, since its performance does not depend on α_1. The last observation is about the difference in the performances between "US" and "OS". Since "US" performance does not change with α_1 whereas "OS" performance improves by decreeasing α_1. It then expected, as in the figure, that for small α_1 "OS" outperforms "US". Whereas, for high α_1 the "US" scheme outperforms the "OS" scheme.

We also evaluate the outage probability performance of all three schemes, i.e., "WSNS", "US", and "OS", versus ϵ in Fig. 8, for different values of α_1. As expected from previous results the "US" scheme does not change with α_1. Also, we note that as α_1 increases both "WSNS" and "OS" outage probability performance increases. It is also noted that for high α_1 "US" outperforms

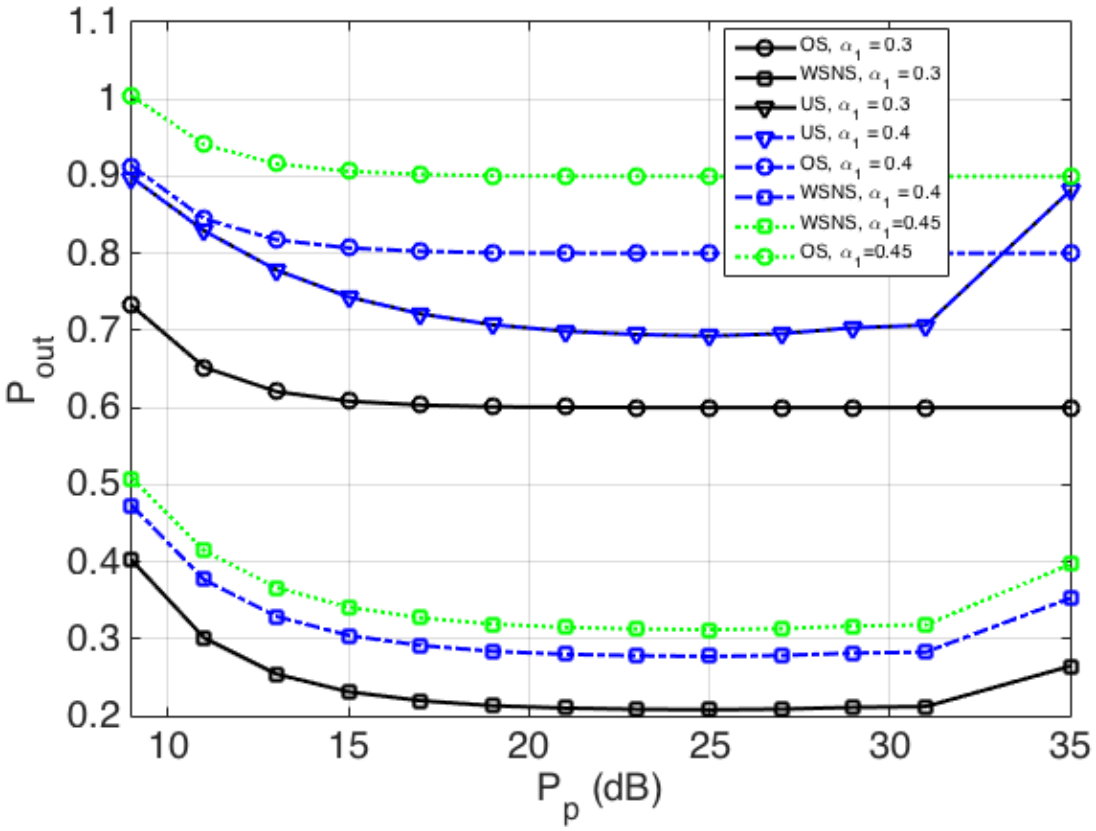

Fig. 7: The outage probability of combined, underlaying, and opportunistic sharing schemes versus $\mathcal{P}_p$, for: $\hat{s}$=30dB, ϵ = 0.4,$R_s = R_p$ = 0.5 symbols/sec, T_c/T = 95%.

"OS", whereas as α_1 goes small then "OS" outperforms "US".

VIII. Conclusion

In this work, we considered a spectrum-sharing model in a block-fading environment. We minimized the outage probability under several constraints including the primary user outage constraint. We derived the exact expressions of the optimal power allocation and the corresponding outage region. The exact solution complexity was illustrated via an example of two communication blocks. Thus, compact formulas for the lower and upper bounds of the targeted outage were provided and the associated sub-optimal power strategies were highlighted. These bounds were shown to be optimal at high SNR in the sense that they both achieve the same diversity order. Also, the system performance under the availability of sensing information was analytically investigated. The corresponding minimum outage region was derived. Numerical

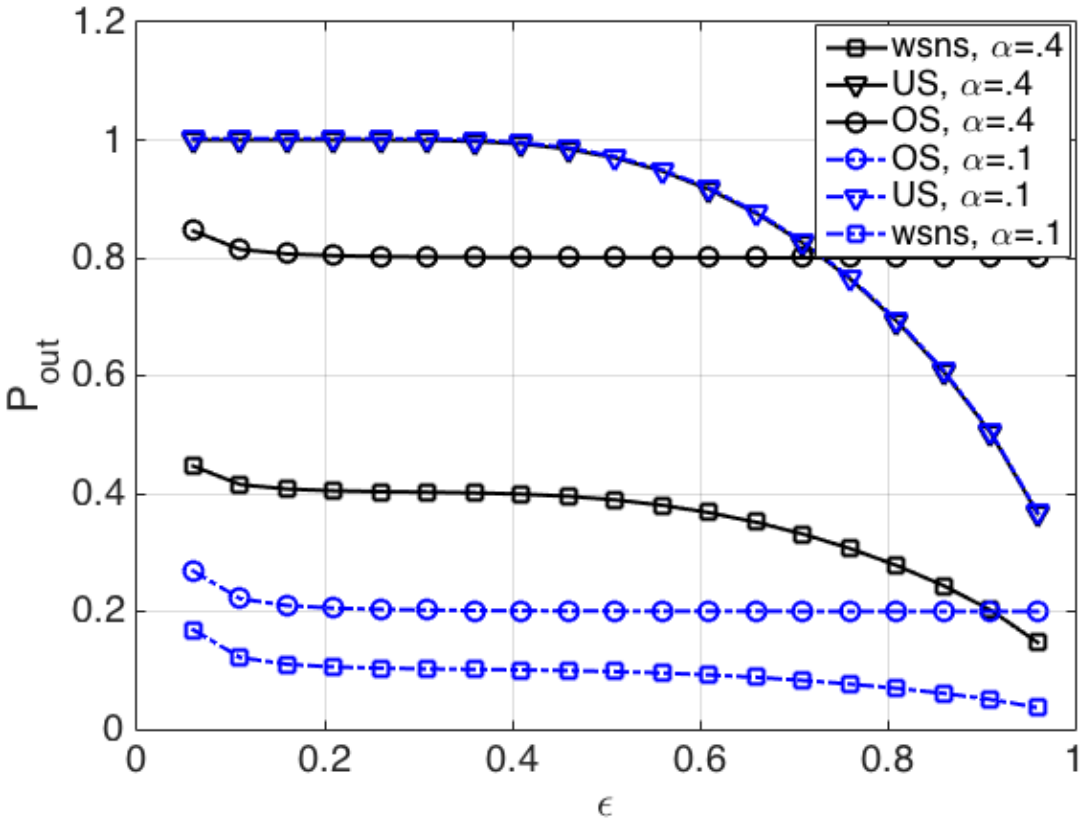

Fig. 8: The outage probability of combined, underlaying, and opportunistic sharing schemes versus ϵ, for: $\hat{s}$ = 35dB, R_s = 1 symbol/sec, T_c/T=95%.

results showed the effect of the cognitive radio constraint on system performance with and without sensing information. We showed that changing the ratio of the cognitive radio constraint to the short-term power constraint affects the convexity property of the outage region.

APPENDIX A

In this appendix, we verify that both regions, $\mathcal{A}$ and $\mathcal{B}$, of $\boldsymbol{\gamma}_s$ do not occur simultaneously given a specific value of $\mathcal{P}_{pu}$. To verify this, we expand both regions $\mathcal{A}$ and $\mathcal{B}$. The original definition of region $\mathcal{A}$ is rewritten as follows,

$$\mathcal{A}=\left\{\boldsymbol{\gamma}_s\in\mathcal{Q}:\mathcal{P}_{pu}\geq\hat{s}\cap\gamma_{s1}>0\cap\frac{\gamma_{s1}P_I}{2\gamma_{s1}\mathcal{P}_{pu}-2\gamma_{s1}\hat{s}+P_I}\leq\gamma_{s2}\leq\gamma_{s1}\right\}, \tag{45}$$

whereas the region $\mathcal{B}$ is expanded as follows,

$$\mathcal{B} = \left\{ \boldsymbol{\gamma}_s \in \mathcal{Q} : 0 < \mathcal{P}_{pu} < \hat{s} \cap \gamma_{s1} > 0 \cap -\frac{\gamma_{s1} P_I}{2\gamma_{s1}\mathcal{P}_{pu} - 2\gamma_{s1}\hat{s} - P_I} < \gamma_{s2} \leq \gamma_{s1} \right\}. \tag{46}$$

From (45), we note that in order for region $\mathcal{A}$ to contribute to the outage the relation between $\hat{s}$ and $\mathcal{P}_{pu}$ has to satisfy $\mathcal{P}_{pu} \geq \hat{s}$. On the other hand, from (46), we note that the relation must be $\mathcal{P}_{pu} < \hat{s}$. Therefore, it is clear that for a certain $\mathcal{P}_{pu}$ and $\hat{s}$, either region $\mathcal{A}$ or region $\mathcal{B}$ can contribute to the outage region, not both of them.

APPENDIX B
DERIVATION OF P^u_{out}

The upper bound on P^+_{out} is derived by considering the selection-combining over the best fading block. In this scheme, communication is performed over a single block (the one with the strongest channel gain). The corresponding outage probability of the selection-combining scheme is derived as follows,

$$P^u_{out} = \Pr\left[\frac{1}{2M} \max_{\boldsymbol{\gamma}_s} \log\left(1 + \frac{M\mathcal{P}_{bd}\gamma_{si}}{(1+\mathcal{P}_p\sigma^2_{ps})}\right) < R_s \right] \tag{47a}$$

$$= \Pr\left[\max_{\boldsymbol{\gamma}_s} \gamma_{si} < \frac{(e^{2MR_s}-1)(1+\mathcal{P}_p\sigma^2_{ps})}{M\mathcal{P}_{bd}} \right] \tag{47b}$$

$$= \left[F_{\gamma_s}\left(\frac{(e^{2MR_s}-1)(1+\mathcal{P}_p\sigma^2_{ps})}{M\mathcal{P}_{bd}} \right) \right]^M, \tag{47c}$$

where (47b) follows from the fact that the logarithm is a monotonically increasing function. Equality (47c) follows because the output of maximum of I.I.D. random variables has the following CDF, $\Pr[\max \gamma_{si} \leq z] = \prod_{i=1}^{M} \Pr[\gamma_{si} \leq z] = \Pr[\gamma_s \leq z]^M$. The function F_{γ_s} is the CDF of the random variable γ_s. Note that, P^u_{out} decreases with $\mathcal{P}_{bd}$ and increases with R_s.

APPENDIX C
ASYMPTOTIC OPTIMAL POWER ASSIGNMENT

In this appendix, we prove that the optimal power assignment at high SINR is a uniform assignment over all transmission blocks. Without loss of generality, we prove the optimal power

allocation at high SINR for $\mathfrak{P}_0$ as follows,

$$\begin{aligned}
P_{out} &\overset{(a)}{=} \lim_{\mathcal{P}_{bd}\to\infty} \min_{\mathbf{p}_s:\langle\mathbf{p}_s\rangle\leq\mathcal{P}_{bd}} M!\Pr\left[\bigcup_{\mu=1}^{M}\left[\mathcal{U}(R_s,\mathcal{P}_{bd})\bigcap\mathcal{V}_\mu\right]\right] \\
&= \lim_{\mathcal{P}_{bd}\to\infty} \min_{\mathbf{p}_s:\langle\mathbf{p}_s\rangle\leq\mathcal{P}_{bd}} M!\Pr[\mathcal{Q}_i=\mathcal{Q}]\sum_{\mu=1}^{M}\Pr[\mu]\Pr\left[\frac{1}{2M}\sum_{m=1}^{\mu}\log\left(1+\gamma_{sm}p_{sm}^{st}(\boldsymbol{\gamma}_s)\right)<R_s\middle|\mu,\mathcal{Q}_i=\mathcal{Q}\right] \\
&\overset{(b)}{=} \lim_{\mathcal{P}_{bd}\to\infty}\sum_{\mu=1}^{M}\Pr[\mu]\Pr\left[\frac{1}{2M}\sum_{m=1}^{\mu}\log\left(1+\gamma_{sm}\left[\frac{1}{\mu}\sum_{l=1}^{\mu}\frac{1}{\gamma_{sl}}+\frac{M}{\mu}\mathcal{P}_{bd}-\frac{1}{\gamma_{sm}}\right]\right)<R_s\middle|\mu,\mathcal{Q}_i\right],
\end{aligned} \tag{48}$$

where $\mathcal{Q}_i$ is defined as the i^{th} way of sorting M variables, $i\in\{1,\ldots,M!\}$ and $\Pr\{\mathcal{Q}_i=\mathcal{Q}\}=\frac{1}{M!}$, and region $\mathcal{Q}$ is defined as in (3). Equality (a) is obtained from the outage region definition in (11). The term $M!$ in (a) represents the number of ways to sort $M!$ numbers. Equality (b) results from expanding p_{sm}^{st} as in (17). It is clear that the term within the brackets $\frac{1}{\mu}\sum_{l=1}^{\mu}\frac{1}{\gamma_{sl}}+\frac{M}{\mu}\mathcal{P}_{bd}-\frac{1}{\gamma_{sm}}\approx\frac{M}{\mu}\mathcal{P}_{bd}$ as $\mathcal{P}_{bd}\to\infty$. It follows that,

$$\begin{aligned}
P_{out} &\approx \lim_{\mathcal{P}_{bd}\to\infty}\sum_{\mu=1}^{M}\Pr[\mu]\Pr\left[\frac{1}{2M}\sum_{m=1}^{\mu}\log\left(1+\gamma_{sm}\left[\frac{M}{\mu}\mathcal{P}_{bd}\right]\right)<R_s\middle|\mu,\mathcal{Q}_i\right] \\
&\overset{(c)}{\approx} \Pr\left[\frac{1}{2M}\sum_{m=1}^{M}\log\left(1+\gamma_{sm}\mathcal{P}_{bd}\right)<R_s\middle|\mu=M,\mathcal{Q}_i\right],
\end{aligned} \tag{49}$$

where (c) follows from the fact that as $\mathcal{P}_{bd}\to\infty$, all the available blocks are used for transmission ($\mu=M$). Then, $\lim_{\mathcal{P}_{bd}\to\infty}\Pr[\mu=M]=\lim_{\mathcal{P}_{bd}\to\infty}\Pr\left[\frac{1}{M}\sum_{l=1}^{M}\frac{1}{\gamma_{sl}}+\mathcal{P}_{bd}\geq\frac{1}{\gamma_{sM}}\right]\approx 1$.

APPENDIX D
ASYMPTOTIC LOWER BOUND ON P_{out}^{+}

The detailed proof of Lemma 3 is provided as follows,

$$P_{out}^{+} \approx \lim_{\mathcal{P}_{bd}\to\infty}\Pr\left[\frac{1}{2M}\sum_{m=1}^{M}\log\left(1+\frac{\mathcal{P}_{bd}\gamma_{si}}{(1+\mathcal{P}_p\sigma_{ps}^2)}\right)<R_s\right] \tag{50a}$$

$$\geq \lim_{\mathcal{P}_{bd}\to\infty}\Pr\left[\log\left(1+\frac{1}{M}\sum_{m=1}^{M}\frac{\mathcal{P}_{bd}\gamma_{si}}{(1+\mathcal{P}_p\sigma_{ps}^2)}\right)<2R_s\right] \tag{50b}$$

$$= \lim_{\mathcal{P}_{bd}\to\infty}\Pr\left[\sum_{i=1}^{M}\gamma_{si}<\frac{M\left(e^{(2R_s)}-1\right)(1+\mathcal{P}_p\sigma_{ps}^2)}{\mathcal{P}_{bd}}\right]=P_{out}^{l,\infty}. \tag{50c}$$

The asymptotic equivalence at (50a) follows from using the optimal power allocation at high budget power. The inequality (50b) follows from Jensen inequality.

APPENDIX E
PROOF OF COROLLARY 1

We begin by proving (30) from left to right. The optimal power solution that achieves minimum outage probability, in (13a), must satisfy the following constraint: $\langle \mathbf{p}_s \rangle \leq s^*$. Therefore, by substituting $\langle \mathbf{p}_s \rangle \leq s^*$ in (5), it follows that,

$$\mathcal{P}^{lt} = \int_{\overline{\mathcal{R}_{cr}}(s^*)} \langle \mathbf{p}_s \rangle dG(\boldsymbol{\gamma}_s) \leq \int_{\overline{\mathcal{R}_{cr}}(s^*)} s^* dG(\boldsymbol{\gamma}_s) = s^* \int_{\overline{\mathcal{R}_{cr}}(s^*)} dG(\boldsymbol{\gamma}_s). \tag{51}$$

Since the integral in the last term in (51) is a probability, then $0 \leq \int_{\overline{\mathcal{R}}(s^*)} dG(\boldsymbol{\gamma}_s) \leq 1$. It follows that, $s^* \geq \mathcal{P}^{lt}$. Hence, it is concluded that $\mathcal{P}^{lt} \to \infty \implies s^* \to \infty$.

To prove the other direction of (30), *i.e.*, $s^* \to \infty \implies \mathcal{P}^{lt} \to \infty$, we assume that $\mathcal{P}_{bd} = s^*$; otherwise the long-term constraint will be inactive and this becomes unnecessary to prove. We note that, at $\mathcal{P}_{bd} \to \infty$, the optimal power is a uniform allocation over all M channels with $p_{si}(\boldsymbol{\gamma}_s) = \mathcal{P}_{bd} = s^*$. The proof of this claim is given in Appendix C. Applying this fact to (5), we obtain,

$$\begin{aligned} \mathcal{P}^{lt} &\approx \lim_{\mathcal{P}_{bd}\to\infty} \mathcal{P}_{bd} \int_{\overline{\mathcal{R}}(\mathcal{P}_{bd})} dG(\boldsymbol{\gamma}_s) = \lim_{\mathcal{P}_{bd}\to\infty} s^* \Pr\left[\boldsymbol{\gamma}_s \in \overline{\mathcal{R}}(\mathcal{P}_{bd})\right] \\ &= s^* \lim_{\mathcal{P}_{bd}\to\infty} \Pr\left[\lambda^{lt}(M, \boldsymbol{\gamma}_s) - \frac{1}{M}\sum_{m=1}^{M} \frac{1}{\gamma_{sm}} \leq \mathcal{P}_{bd}\right] \approx s^*. \end{aligned} \tag{52}$$

It follows that $s^* \to \infty \implies \mathcal{P}^{lt} \to \infty$, which completes the proof of (30).

APPENDIX F
PROOF OF COROLLARY 2

In this appendix we provide a proof for Corollary 2. The flow of this proof is similar to the lines provided in the sketch proof of Corollary 2. That is, we begin by verifying that the diversity order of the upper and lower bounds of the system are equivalent. We then shows that this diversity order is equivalent to the no-interference case (no CR environment).

The diversity order of P_{out}^{u}, called d_l^-, is derived using the above definition, i.e., $d_{out} = -\lim_{\mathcal{P}_{bd}\to\infty} \frac{\log(P_{out})}{\log(\mathcal{P}_{bd})}$, while replacing P_{out} by P_{out}^{u}. The diversity order, d_l^-, is derived as follows,

$$d_l^- = -\lim_{\mathcal{P}_{bd}\to\infty} \frac{\log\left[1 - e^{(-C)}\right]^M}{\log\left(\mathcal{P}_{bd}\right)} \approx -\lim_{\mathcal{P}_{bd}\to\infty} \frac{M \log\left[C\right]}{\log(\mathcal{P}_{bd})} = M, \tag{53}$$

where $C = \frac{(e^{(2MR_s)}-1)(1+\mathcal{P}_p\sigma_{ps}^2)}{M\mathcal{P}_{bd}}$. The approximation is derived by Taylor expansion of the exponential function in the previous step. Note that the term inside the exponential $\frac{(e^{(2MR_s)}-1)(1+\mathcal{P}_p\sigma_{ps}^2)}{M\mathcal{P}_{bd}}$ $\to 0$ as $\mathcal{P}_{bd} \to \infty$.

Hereafter, we derive the diversity order of the lower bound of P_{out}^{+}. This derivation is divided into two parts. The first part addresses the diversity order of the asymptotic lower bound, derived in (29), called $d_{u,\infty}^{-}$. The second part addresses the diversity order of a general (non-asymptotic) lower bound outage probability $\left(P_{out}^{l}\right)$, called d_{u}^{-}. This part is addressed in Appendix G (to avoid interrupting the flow of the proof), in which we prove that $d_{u}^{-} = M$.

The diversity order of the outage probability in (29) is obtained as follows,

$$
\begin{aligned}
d_{u,\infty}^{-} &= \lim_{\mathcal{P}_{bd}\to\infty} -\frac{1}{\log(\mathcal{P}_{bd})} \log\left(\frac{\gamma\left(M,z\right)}{\Gamma(M)}\right) && \text{(54a)}\\
&= \lim_{\mathcal{P}_{bd}\to\infty} -\frac{1}{\log(\mathcal{P}_{bd})} \log\left[\frac{\left(z\right)^{M}}{(M-1)!}\sum_{n=0}^{\infty}\left(\frac{(-1)^{n}\left(z\right)^{n}}{(M+n)n!}\right)\right] && \text{(54b)}\\
&\approx \lim_{\mathcal{P}_{bd}\to\infty} -\frac{1}{\log(\mathcal{P}_{bd})} \log\left(\frac{\left(z\right)^{M}}{M!}\right) && \text{(54c)}\\
&\leq \lim_{\mathcal{P}_{bd}\to\infty} -\frac{M\log\left(z\right)-\log\left(M!\right)}{\log(\mathcal{P}_{bd})} = M, && \text{(54d)}
\end{aligned}
$$

where $z = \frac{M\left(e^{(2R_s)}-1\right)(1+\mathcal{P}_p\sigma_{ps}^2)}{\mathcal{P}_{bd}}$, the function $\gamma(M,z) = \int_0^z t^{M-1}e^{-t}dt$ is the lower incomplete Gamma function, and $\Gamma(M) = (M-1)!$ is the Gamma function. Equality (54a) is obtained by observing that the sum of exponential random variables follows an Erlang distribution with parameter $\lambda = 1$ and shape parameter $k = M$ (this is a special case of Chi-square distribution with $2M$ degrees of freedom). The equality (54b) follows by applying Taylor expansion to the lower incomplete Gamma function. The asymptotic equivalence in (54c) follows by ignoring $n \geq 1$ because, asymptotically, as $z \to 0$, the first term corresponding to $n = 0$ dominates the sum. The final result in (54d) shows that the diversity order of $P_{out}^{l,\infty}$ is equivalent to the one derived in (53). Note that the diversity order of the asymptotic lower bound ($P_{out}^{l,\infty}$) and the non-asymptotic lower bound (P_{out}^{l}) on P_{out}^{+} are $d_{u,\infty}^{-} = d_{u}^{-} = M$.

By comparing (53) and (54), we note that, $M = d_{l}^{-} \leq d_{out}^{-} \leq d_{u,\infty}^{-} = M$, thus, $d_{out}^{-} = M$.

It is known that the diversity order does not improve by introducing interference to the SU system. We therefore consider the diversity order of a point-to-point communication system in

[5] (noted as d_{out}^{+}) as an upper bound to the exact outage probability of the proposed system, not P_{out}^{+}. Recall that in [5] the authors do not consider the interference from PU to SU. We find that, $d_{out} \leq d_{out}^{+} = M$.

Comparing d_{out}^{-} and d_{out}^{+}, we note that the exact diversity order of the proposed system is bounded as $d_{out}^{-} \leq d_{out} \leq d_{out}^{+}$, thus, $d_{out} = M$. This concludes the proof of Corollary 2.

APPENDIX G
DERIVATION OF P_{out}^{l} AND $d_{u,\infty}^{-}$

In this appendix, we derive a lower bound on the outage probability, P_{out}^{+}, and the corresponding diversity order. The lower bound on P_{out}^{+} is derived using the original definition of P_{out}^{+} as follows,

$$P_{out}^{+} = \Pr\left[\frac{1}{2M}\sum_{i=1}^{M}\log\left(1+\frac{p_{si}(\boldsymbol{\gamma}_s)\gamma_{si}}{1+\mathcal{P}_p\sigma_{ps}^2}\right) < R_s\right] \tag{55a}$$

$$\geq \Pr\left[\log\left(1+\frac{1}{M}\sum_{i=1}^{M}\frac{p_{si}(\boldsymbol{\gamma}_s)\gamma_{si}}{1+\mathcal{P}_p\sigma_{ps}^2}\right) < 2R_s\right] \tag{55b}$$

$$\geq \Pr\left[\frac{\gamma_s^{max}}{M}\frac{1}{1+\mathcal{P}_p\sigma_{ps}^2}\sum_{i=1}^{M}p_{si}(\boldsymbol{\gamma}_s) < e^{(2R_s)}-1\right] \tag{55c}$$

$$\geq \Pr\left[\gamma_s^{max}\frac{\min\left(\mathcal{P}_{pu},\mathcal{P}^{st},s^*\right)}{(1+\mathcal{P}_p\sigma_{ps}^2)} < \left(e^{(2R_s)}-1\right)\right] \tag{55d}$$

$$= \left[F_{\gamma_s}\left(\frac{(e^{(2R_s)}-1)(1+\mathcal{P}_p\sigma_{ps}^2)}{\mathcal{P}_{bd}}\right)\right]^{M} = P_{out}^{l}, \tag{55e}$$

where (55b) is obtained using the Jensen inequality. The inequality (55c) follows from the fact that $\gamma_s^{max}\frac{1}{M}\sum_{i=1}^{M}p_{si}(\boldsymbol{\gamma}_s) \geq \frac{1}{M}\sum_{i=1}^{M}p_{si}(\boldsymbol{\gamma}_s)\gamma_{si}$, where γ_s^{max} is defined as $\gamma_s^{max} = \max_{\boldsymbol{\gamma}_s}\boldsymbol{\gamma}_s$. The term in (55d) is a relaxed version of the one in (55c); hence, the relaxed one achieves lower outage probability. The equality (55e) results in the CDF of the maximum of I.I.D. random variables. The function F_{γ_s} is the CDF of the random variable γ_s. Thus, $F_{\gamma_s}(.)$ is a monotonic, non-decreasing function of its argument. Therefore, it is noted that P_{out}^{l} decreases with both M and $\mathcal{P}_{bd}$, and increases with R_s. The associated diversity order of P_{out}^{l}, in (55e), is derived as,

$$d_u^{-} = -\lim_{\mathcal{P}_{bd}\to\infty}\frac{M\log\left[1-e^{\left(-\frac{(e^{(2R_s)}-1)(1+\mathcal{P}_p\sigma_{ps}^2)}{\mathcal{P}_{bd}}\right)}\right]}{\log(\mathcal{P}_{bd})} = M. \tag{56}$$

We note that this diversity order is equivalent to $d^{-}_{u,\infty}$.

APPENDIX H

In this appendix, we prove that if $\mathcal{O}_\lambda \subset \mathcal{O}$ then (40) is satisfied. Let us rewrite the region $\mathcal{O}$ as $\mathcal{O} = \mathcal{O}_\lambda \cup \mathcal{O}_\lambda^-$, where region $\mathcal{O}_\lambda^-$ is a non-empty region. Then, it is easy to see that $\Pr\{\mathcal{O}\} = \Pr\{\mathcal{O}_\lambda\} + \Pr\{\mathcal{O}_\lambda^-\}$. Since region $\mathcal{O}_\lambda^-$ is non-empty, then it is clear that $\Pr\{\mathcal{O}\} > \Pr\{\mathcal{O}_\lambda\}$. This concludes the proof given that it is sufficient to verify that $\mathcal{O}_\lambda \subset \mathcal{O}$ in order to verify (40).

REFERENCES

[1] "Voice and video calling over lte (VoLTE)," White Paper, Ericsson, 2014.

[2] L. Ozarow, S. Shamai, and A. Wyner, "Information theoretic considerations for cellular mobile radio," *IEEE Transactions on Vehicular Technology*, vol. 43, no. 2, pp. 359–378, 1994.

[3] V. Lau, Y. Liu, and T.-A. Chen, "On the design of MIMO block-fading channels with feedback-link capacity constraint," *IEEE Transactions on Communications*, vol. 52, no. 1, pp. 62–70, Jan 2004.

[4] W. Yang, G. Durisi, and E. Riegler, "On the capacity of large-MIMO block-fading channels," *IEEE Journal on Selected Areas in Communications*, vol. 31, no. 2, pp. 117–132, February 2013.

[5] G. Caire, G. Taricco, and E. Biglieri, "Optimum power control over fading channels," *IEEE Transactions on Information Theory*, vol. 45, no. 5, pp. 1468–1489, 1999.

[6] A. Goldsmith, S. Jafar, I. Maric, and S. Srinivasa, "Breaking spectrum gridlock with cognitive radios: An information theoretic perspective," *Proceedings of the IEEE*, vol. 97, no. 5, pp. 894–914, 2009.

[7] I. F. Akyildiz, W.-Y. Lee, M. C. Vuran, and S. Mohanty, "Next generation/dynamic spectrum access/cognitive radio wireless networks: A survey," *Computer Networks*, vol. 50, no. 13, pp. 2127 – 2159, 2006.

[8] T. C. Clancy, "Formalizing the interference temperature model," *Wireless Communications and Mobile Computing*, vol. 7, no. 9, pp. 1077–1086, 2007. [Online]. Available: http://dx.doi.org/10.1002/wcm.482

[9] "IEEE standard for information technology–telecommunications and information exchange between systems–local and metropolitan area networks–specific requirements part 22.1: Standard to enhance harmful interference protection for low-power licensed devices operating in tv broadcast bands," *IEEE Std 802.22.1-2010*, pp. 1–145, 2010.

[10] T. Weiss and F. Jondral, "Spectrum pooling: an innovative strategy for the enhancement of spectrum efficiency," *IEEE Communications Magazine*, vol. 42, no. 3, pp. S8–14, 2004.

[11] G. Bansal, J. Hossain, and V. Bhargava, "Optimal and suboptimal power allocation schemes for OFDM-based cognitive radio systems," *IEEE Transactions on Wireless Communications*, vol. 7, no. 11, pp. 4710–4718, 2008.

[12] P. Wang, M. Zhao, L. Xiao, S. Zhou, and J. Wang, "Power allocation in OFDM-based cognitive radio systems," in *Global Telecommunications Conference, 2007. GLOBECOM '07. IEEE*, 2007, pp. 4061–4065.

[13] X. Kang, H. Garg, Y.-C. Liang, and R. Zhang, "Optimal power allocation for OFDM-based cognitive radio with new primary transmission protection criteria," *IEEE Transactions on Wireless Communications*, vol. 9, no. 6, pp. 2066–2075, 2010.

[14] E. Biglieri, G. Caire, and G. Taricco, "Limiting performance of block-fading channels with multiple antennas," *IEEE Transactions on Information Theory*, vol. 47, no. 4, pp. 1273–1289, 2001.

[15] J. Chen and K.-K. Wong, "Communication with causal CSI and controlled information outage," *IEEE Transactions on Wireless Communications*, vol. 8, no. 5, pp. 2221–2229, 2009.

[16] F. Khan, T. Ratnarajah, M. Sellathurai, and S. Prakriya, "Outage analysis of causal cognitive radio channel," in *2009 First UK-India International Workshop on Cognitive Wireless Systems (UKIWCWS)*, 2009, pp. 1–6.

[17] A. Limmanee, S. Dey, and J. Evans, "Service-outage capacity maximization in cognitive radio for parallel fading channels," *IEEE Transactions on Communications*, vol. 61, no. 2, pp. 507–520, 2013.

[18] X. Kang, R. Zhang, Y.-C. Liang, and H. K. Garg, "Optimal power allocation strategies for fading cognitive radio channels with primary user outage constraint," *IEEE Journal on Selected Areas in Communications*, vol. 29, no. 2, pp. 374–383, February 2011.

[19] D. Xu, Z. Feng, Y. Li, and P. Zhang, "Outage probability minimizing power/rate control for cognitive radio multicast networks," in *IEEE Global Telecommunications Conference (GLOBECOM 2011)*, Dec 2011, pp. 1–6.

[20] Y. Zou, Y.-D. Yao, and B. Zheng, "Outage probability analysis of cognitive transmissions: Impact of spectrum sensing overhead," *IEEE Transactions on Wireless Communications*, vol. 9, no. 8, pp. 2676–2688, August 2010.

[21] P. Wang and P.-Y. Kam, "Feedback power control with bit error outage probability QoS measure on the Rayleigh fading channel," *IEEE Transactions on Communications*, vol. 61, no. 4, pp. 1621–1631, April 2013.

[22] J. Luo, R. Yates, and P. Spasojevic, "Service outage based power and rate allocation for parallel fading channels," *IEEE Transactions on Information Theory*, vol. 51, no. 7, pp. 2594–2611, 2005.

[23] M. Medard, "The effect upon channel capacity in wireless communications of perfect and imperfect knowledge of the channel," *IEEE Transactions on Information Theory*, vol. 46, no. 3, pp. 933–946, 2000.

[24] Z. Rezki and M.-S. Alouini, "On the outage capacity of the block fading channel at low-power regime," in *IEEE International Symposium on Information Theory (ISIT), 2014*, June 2014, pp. 2894–2898.

[25] L. Grippo and M. Sciandrone, "On the convergence of the block nonlinear Gauss-Seidel method under convex constraints," *Operations Research Letters*, vol. 26, no. 3, pp. 127 – 136, 2000.

[26] R. W. Yeung, *A First Course in Information Theory (Information Technology: Transmission, Processing and Storage)*. Secaucus, NJ, USA: Springer-Verlag New York, Inc., 2006.

[27] A. Cambini and L. Martein, *Generalized Convexity and Optimization: Theory and Applications*. Springer, 2008.